Paleostress field reconstruction and revised tectonic history of the Donbas fold and thrust belt (Ukraine and Russia).

Saintot, A.N.; Stephenson, R.A.; Brem, A; Stovba, S.; Privalov, V.

published in
Tectonics
2003

DOI (link to publisher)
10.1029/2002TC001366

document version
Publisher's PDF, also known as Version of record

Paleostress field reconstruction and revised tectonic history of the Donbas fold and thrust belt (Ukraine and Russia)

Aline Saintot, Randell Stephenson, and Arjan Brem

Faculty of Earth and Life Sciences, Vrije Universiteit, Amsterdam, Netherlands

Sergiy Stovba

Technology Centre, Ukrgeofisika, Kyiv, Ukraine

Vitaliy Privalov

Faculty of Mining and Geology, Donetsk State Technical University, Donetsk, Ukraine

Received 15 February 2002; revised 17 June 2003; accepted 20 June 2003; published 25 October 2003.

[1] In the WNW-ESE Donbas fold belt (DF), inversion of 3500 microtectonic data collected at 135 sites, in Proterozoic, Devonian, Carboniferous, and Cretaceous competent rocks allowed reconstruction of 123 local stress states. Accordingly, four successive paleostress fields reveal the tectonic evolution of the DF. At the numerous sites that have been affected by polyphase tectonics, the chronology between local paleostress states (also paleostress fields) was established using classical criteria (crosscutting striae, pre- or post-folding stress states, stratigraphic control). The oldest event is an extensional stress field with NNE-SSW σ_3. It corresponds to the rifting phases that generated the basin in Devonian times and its early Visean reactivation. Later, the DF was affected by a transtension, with NW-SE σ_3 characterizing Early Permian tectonism, including the development of the "Main Anticline" of the DF and the pronounced uplift of its southern margin and Ukrainian Shield. Two paleostress fields characterize the Cretaceous/Paleocene inversion of the DF, which was accompanied by folding and thrusting. Both are compressional in type but differ by the trend of σ_1, which was first NW-SE and subsequently N-S. The discrete paleostress history of the DF allows a revised interpretation of its tectonic evolution with significant implications for understanding the geodynamic evolution of the southern margin of the East European Craton. *INDEX TERMS:* 8105 Tectonophysics: Continental margins and sedimentary basins (1212); 8110 Tectonophysics: Continental tectonics—general (0905); 8164 Tectonophysics: Stresses—crust and lithosphere; 8005 Structural Geology: Folds and folding; 8010 Structural Geology: Fractures and faults; *KEYWORDS:* Dnieper-Donets Basin, Donbas fold belt, paleostress, East European Craton. **Citation:** Saintot, A., R. Stephenson, A. Brem, S. Stovba, and V. Privalov, Paleostress field reconstruction and revised tectonic history of the Donbas fold and thrust belt (Ukraine and Russia), *Tectonics*, *22*(5), 1059, doi:10.1029/2002TC001366, 2003.

0278-7407/03/2002TC001366$12.00

1. Introduction

[2] The Donbas fold and thrust belt (DF) is the strongly inverted and compressionally deformed part of the Dnieper-Donets Basin (DDB), a Late Devonian rift basin located on the southwestern part of the East European Craton (EEC), in eastern Ukraine and in southern Russia (Figure 1a). Further to the southeast the DF joins the contiguous, deformed southern margin of the EEC (Karpinsky Swell). The width of the original rift basin (shaded in Figure 1a) varies between 60–70 in the northwest and 140–160 km in the southeast. Thicknesses of the Late Palaeozoic and younger sedimentary succession increase from only about 2 km in the northwest to about 23 km in the DF and most of this is of Carboniferous age [e.g., *Chekunov et al.*, 1993; *Chekunov*, 1994]. Devonian rifting was accompanied by major magmatic activity and the uplift of the Ukrainian Shield and the Voronezh Massif, forming a large radius arch that is transected by the DDB [*Gavrish*, 1989; *Wilson and Lyashkevich*, 1996].

[3] There are profound along strike variations in the degree of basin "inversion" in the DDB, ranging from severe in the DF to practically none in the Dnieper segment [*Chirvinskaya and Sollogub*, 1980; *Stephenson et al.*, 2001]. There is a major Permian unconformity, with increasing thicknesses of eroded strata inferred to the southeast, and it has long been regarded that basin "inversion" was related to Permian Variscan/Uralian orogenesis on the margins of the EEC [e.g., *Milanovsky*, 1992] or to the activity of an asthenospheric (mantle) diapir [*Gavrish*, 1985, 1989; *Chekunov*, 1994]. Several kilometers of mainly Carboniferous strata have been eroded in the DF, especially on its southern margin [e.g., *Stovba and Stephenson*, 1999]. What is known about the subsurface structure of the DF has been based on surface exposure, shallow boreholes and deep sounding profiles [*Stovba and Stephenson*, 1999], to be presently augmented by new deep seismic reflection data still being interpreted [*Roy-Chowdhury et al.*, 2001].

[4] The driving mechanism of rifting causing the DDB remains a matter of speculation [*Stephenson et al.*, 2001]

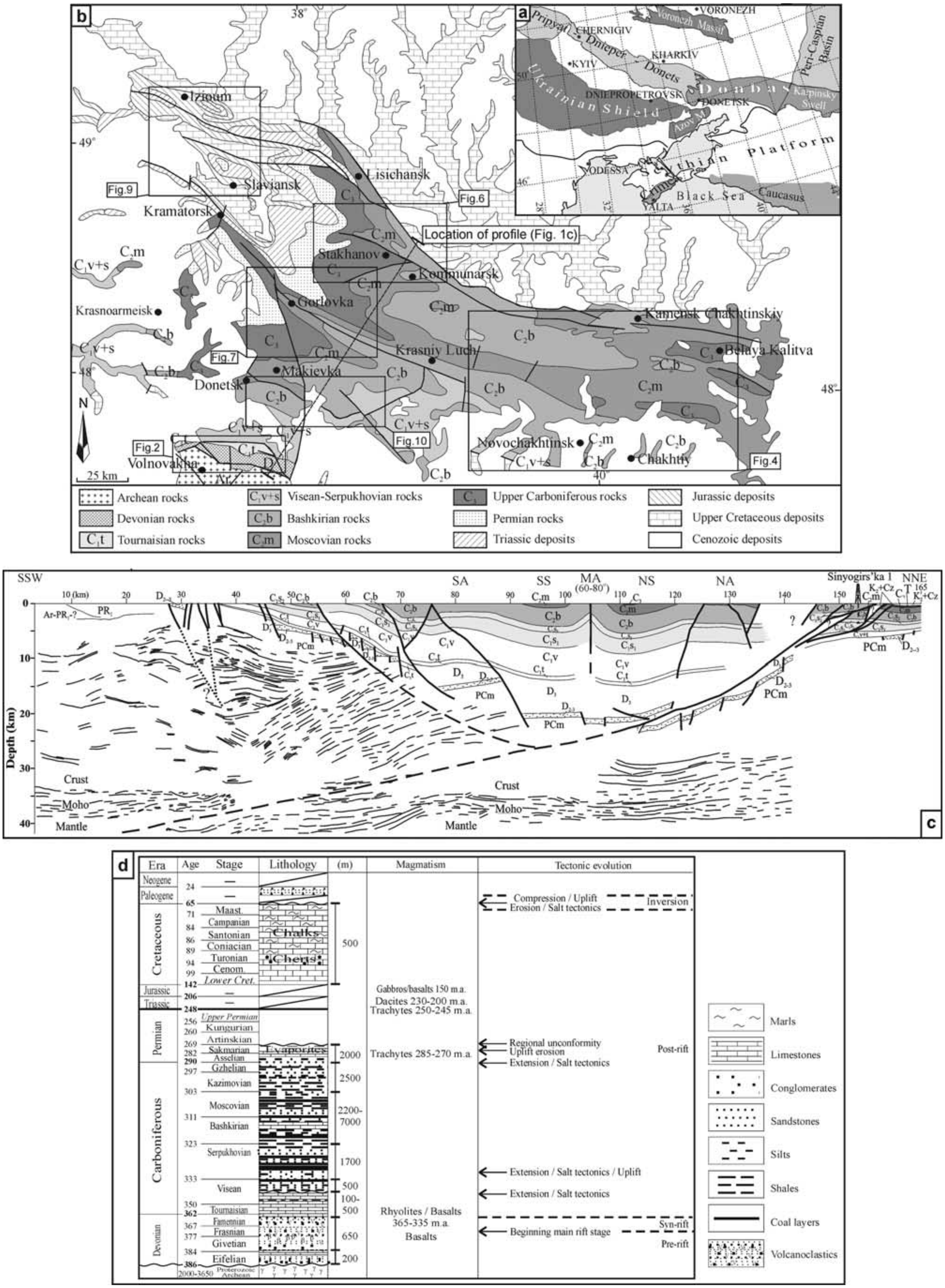
b
a
VORONEZH
Voronezh Massif
Pripyat
CHERNIGIV
Dnieper
KHARKIV
KYIV
Donets
Peri-Caspian Basin
Ukrainian Shield
DNIEPROPETROVSK
Donbas
DONETSK
Karpinsky Swell
Azov M.
Scythian Platform
ODESSA
Crimea
Black Sea
Caucasus
YALTA
Izioum
Slaviansk
Lisichansk
Kramatorsk
Fig.9
Fig.6
Location of profile (Fig. 1c)
Stakhanov
Kommunarsk
Gorlovka
Krasnoarmeisk
Kamensk Chakhtinskiy
Krasniy Luch
Belaya Kalitva
Fig.7
Makievka
Donetsk
Novochakhtinsk
Chakhtiy
Fig.2
Volnovakha
Fig.10
Fig.4
25 km
N
Archean rocks
Devonian rocks
Tournaisian rocks
Visean-Serpukhovian rocks
Bashkirian rocks
Moscovian rocks
Upper Carboniferous rocks
Permian rocks
Triassic deposits
Jurassic deposits
Upper Cretaceous deposits
Cenozoic deposits
SSW
SA
SS
MA (60-80°)
NS
NA
Sinyogirs'ka 1
NNE
Depth (km)
Crust
Moho
Mantle
c
d
Era
Age
Stage
Lithology
(m)
Magmatism
Tectonic evolution
Neogene
Paleogene
Cretaceous
Jurassic
Triassic
Permian
Carboniferous
Devonian
Maast.
Campanian
Santonian
Coniacian
Turonian
Cenom.
Lower Cret.
Chalks
Cherts
Upper Permian
Kungurian
Artinskian
Sakmarian
Asselian
Evaporites
Gzhelian
Kazimovian
Moscovian
Bashkirian
Serpukhovian
Visean
Tournaisian
Famennian
Frasnian
Givetian
Eifelian
Proterozoic Archean
Compression / Uplift
Erosion / Salt tectonics
Inversion
Gabbros/basalts 150 m.a.
Dacites 230-200 m.a.
Trachytes 250-245 m.a.
Regional unconformity
Uplift erosion
Extension / Salt tectonics
Trachytes 285-270 m.a.
Post-rift
Extension / Salt tectonics / Uplift
Extension / Salt tectonics
Rhyolites / Basalts 365-335 m.a.
Basalts
Beginning main rift stage
Syn-rift
Pre-rift
Marls
Limestones
Conglomerates
Sandstones
Silts
Shales
Coal layers
Volcanoclastics

and, similarly, the mechanisms leading to uplift and compressional deformation in the inverted (DF) part of the DDB are also problematic. The geological setting of the DF is complicated by the increasing proximity of the basin axis to the inferred southern edge of the EEC and its presumed relationship with contemporaneous basin development on the southern margin of the EEC. Recently, *Stovba and Stephenson* [1999] presented seismic reflection data in the southeastern DDB (Donets segment) documenting that Late Palaeozoic reactivations (syn-Variscan/Uralian) were (trans)tensional rather than compressional, while those at the end of the Triassic and at the end of the Cretaceous were compressional in nature. Post-rift reactivations increase toward the southeast and *Stovba and Stephenson* [1999] surmised that they must be even more profound in the DF than in the uninverted part of the DDB. Accordingly, *Stovba and Stephenson* [1999] concluded that the main phases of shortening in the DF were Cimmerian (Late Triassic-Jurassic) and Eo-Alpine (end Cretaceous). This was in contradiction to firmly entrenched, long-held concepts prevalent in all published materials on the DF that it forms a part of an external Variscan (Hercynian) foldbelt ringing the southern margin of the European craton from western Europe to the Urals [*Popov*, 1963; *Milanovsky*, 1992].

[5] This paper presents an attempt to test the hypothesis of *Stovba and Stephenson* [1999] by applying modern methods of paleostress analysis [*Angelier*, 1990, 1994] from microscale brittle structures observable in the exposed geological strata of the DF. These data have permitted a comprehensive characterization of up to four distinct tectonic events, i.e., stress fields, that affected the Late Devonian and younger sedimentary rocks of DF and provide independent support of the viability of the *Stovba and Stephenson* [1999] hypothesis. As such, all paleotectonic concepts of the Variscan evolution of the European continent, at least in respect of its southeastern margin, demand careful reconsideration and likely modification. Any such modification will have important implications for understanding the history of the Paleo-Tethys Ocean and the geodynamic processes that governed its evolution during the Late Palaeozoic.

2. Geology of the Donbas Fold Belt

2.1. Basin Fill

[6] The Devonian to Carboniferous sedimentary succession, deeply buried in other parts of the DDB, is well exposed in the DF (Figure 1b). These sequences have been studied from surface outcrops and coal prospecting boreholes to depths of 1–3 km [*Levenshtein*, 1963; *Popov*, 1963; *Maidanovich and Radzivill*, 1984].

[7] Extensively observed Middle/Late Devonian to Early Carboniferous rocks crop out on the southwestern margin of the DF where they unconformably overlie crystalline basement of the Azov Massif (Figures 1a and 1b). E-W-trending grabens and half-grabens developed possibly as early, but certainly by the end of the Frasnian, and a continental (fluvial, lacustrine) succession was established. Early synrift activity was accompanied by the extrusion of basalts. The Middle/Upper Devonian succession comprises thick clastic and carbonate sediments with interbedded volcanics (1800 m thick, depending on local variations in the quantity of volcanics). The thickness of the Devonian sediments within the axial zone of the DF is thought to be as great as 5 km [*Garkalenko et al.*, 1971; *Borodulin*, 1974] (Figure 1c).

[8] A broad carbonate platform was established across the region from the latest Devonian, until the late early Visean (1000 m thick, Figure 1d). Otherwise, Carboniferous basin development occurred in a post-rift regime of frequent relative sea-level oscillations leading to continuous rhythmic sedimentation of alternating shallow-water, littoral, off-shore and continental facies, including erosional hiatuses [e.g., *Levenshtein*, 1963; *Dvorjanin et al.*, 1996; *Izart et al.*, 1996] (Figure 1d). Late Visean sediments consist mainly of thick sandy-clay deposits interbedded with thin coal and limestone beds. The very thick Middle and Upper Carboniferous strata consist of arenaceous-argillaceous rocks interbedded with coal and limestone beds (Figures 1b, 1c, and 1d).

[9] No Permian sediments are preserved within the DF itself but Early Permian sediments do occur nearby, along the northwestern margin of the DF in its transition to the DDB. They comprise coastal-continental and occasionally shallow-marine facies, represented by monotonous sand-shale series with sparse interbeds of limestones, coals and salt layers. Magmatic rocks of Early Permian age occur in the southwestern DF [*Alexandre et al.*, 2003] (Figure 1d).

[10] Very little Mesozoic sediment is preserved within the DF. In the nearby part of the DDB the Mesozoic succession consists of marine and continental sediments described as "close to" platform type [*Eisenverg*, 1988]. In the western part of the northern margin of the DF, Triassic sediments up to 150–200 m thick are preserved in a narrow strip [*Belov*, 1970]. Jurassic sediments are absolutely absent in the same area [*Popov*, 1963; *Chirvinskaya and Sollogub*, 1980]. In

Figure 1. (opposite) Presentation of the Donbas fold belt. (a) Location of the Donbas in the regional East European structural framework [from *Stovba and Stephenson*, 1999]. (b) Geological map of the Donbas from *Nalivkin* [1983]. (c) Geological cross section constructed from surface geology and shallow boreholes plus depth-converted DOBREflection-2000 seismic profile and southernmost part of the seismic profile extension in 2001, located on Figure 1b [from *Maystrenko et al.*, 2003]; MA (60°–80°): Main Anticline and dips of beds of the two limbs; SS: Southern Syncline; SA: Southern Anticline; NS: Northern Syncline; NA: Northern Anticline. (d) Stratigraphic column of the DF with lithologies, thicknesses, magmatic events with new Ar-Ar absolute ages [from *Alexandre et al.*, 2003], and tectonic evolution from *Stovba and Stephenson*, 1999. (Stratigraphic limits according to the International Stratigraphic Chart, International Union of Geological Sciences: International Commission on Stratigraphy and Commission of the Geological Map of the World, UNESCO, available at http://www.cgmw.org.)

the southwestern part of the DF, Early and Late Triassic and Late Jurassic magmatic rocks crop out [*Chekunov and Naumenko*, 1982; *Alexandre et al.*, 2003] (Figure 1d). On the southern margin of the DF the Mesozoic is represented by up to 500 m of Upper Cretaceous marls and chalks, unconformably overlying either Palaeozoic rocks or crystalline basement (Figure 1b). Angular unconformities within the Mesozoic succession, in particular at the Triassic/Jurassic and Jurassic/Cretaceous boundaries, have been documented on the northwestern margin of the DF [*Konashov*, 1980; *Eisenverg*, 1988]. Palaeogene (sands, clays, marls) and Neogene (sands with clayey interbeds) units, unconformably overlies the Upper Cretaceous and older rocks [*Eisenverg*, 1988].

2.2. Basin Deformation

[11] Deep WNW-ESE faults form the southern and northern boundaries of the DF [*Sollogub et al.*, 1977] (Figures 1b and 1c). Folds in the central part of the DF trend west-northwestward, and are fairly tight, in some places overturned. The Main Anticline (MA) is the largest and most pervasive fold in this zone (Figures 1b and 1c). It is an almost symmetric structure with steeply dipping limbs (60°–80°; Figure 1c), complicated by faults as thrusts (or oblique thrusts), as oblique normal and strike-slip faults developed at its hinge [*Lutuguin*, 1956], in which dextral movement has been recognized [*Maidanovich and Radzivill*, 1984; *Belichenko et al.*, 1999; *Privalov et al.*, 2000]. The MA is bordered by two gentle synclines and anticlines (Figures 1b and 1c). Localized folds and thrust faults (as mesoscale structures) are developed in the northern zone of the DF. Carboniferous strata typically dip at angles of 30°, locally to more than 40°. Many folds are tilted northward. Thrust faulting is more regionalized; some thrusts can be traced for many tens of kilometers. Thrust surfaces commonly dip 40°–60° southward. A set of major north-vergent thrusts characterizes the present-day structure of the northern margin of the DF [*Belokon*, 1975; *Mikhalev and Borodulin*, 1976] (Figure 1c). Stratigraphic offsets on thrust faults can be substantial (1000 to 2000 m); the maximum is 4000 m [*Popov*, 1963]. According to *Popov* [1963] and *Zhykalyak et al.* [2000], thrusting was episodic, with movements occurring during major tectonic phases at the end of Palaeozoic, in the Mesozoic, and the Cenozoic. To the northwest, toward the uninverted part of the Donets segment, offsets on thrusts decrease and fade out. In the southern zone of the DF, E-W trending minor folds prevail. Near the city of Donetsk (cf. Figure 1b) is a zone of transverse structures [*Popov*, 1963]. The gentle WNW-ESE folds are overprinted by a widely developed system of strongly asymmetric folds striking northwest, which over long distances possess the characteristics of flexures. Thrust or reverse faults are south vergent. Faults and block structures occur mainly in a corridor between the DF and Azov Massif. Because most of the area is covered with Upper Cretaceous sediments, they are well studied only in the southwestern DF, where Devonian and Lower Carboniferous sediments crop out (Figure 1b). This zone has the appearance of an undulating, northward dipping monocline broken by series of moderately large faults that produce its block structure. Offsets are 400 m and more; dip angles are to 40°–70°, mostly to the southwest (opposite the dip direction of sedimentary horizons). Individual blocks strike mainly to the northwest, subparallel to the main linear folds of the DF.

[12] The main structures of the DF, in particular the MA, are believed to continue eastward, below Mesozoic platform cover in the area of the Karpinsky Swell [e.g., *Popov*, 1963; *Belov*, 1970; *Garetsky*, 1972] (cf. Figure 1a). The morphology of the eroded surface and the gentle structure of the overlying Jurassic and Cretaceous sedimentary cover are thought to reflect inheritance of the strike and character of the folds observed in the DF. It has also been speculated that the Donbas folds and marginal faults can be traced through the Karpinsky Swell to the Caspian Sea [e.g., *Belov*, 1970; *Garetsky*, 1972] (cf. Figure 1a).

[13] The characteristics and the timing of the tectonic events forming the DF are controversial [cf. *Stovba and Stephenson*, 1999; *Stephenson et al.*, 2001]. Initial rifting was clearly Devonian in age, but the rifting regime as extensional or transtensional is not known. From observations of the orientations of dykes, mainly from the Azov Massif and thought to be related to the Devonian rifting phase [*Muratov*, 1972], as well as fractures in the Devonian volcanics of the DF, *Korchemagin and Yemets* [1987] determined a NNE extensional axis. This was followed by profound post-rift subsidence in the DF during the Carboniferous, as it did in the adjacent DDB, interrupted by rifting phases in late early Visean and in Serpukhovian times [cf. *Stovba et al.*, 1996; *van Wees et al.*, 1996; *Stovba and Stephenson*, 1999] (Figure 1d). Evidence of the former is amply manifested near the southern margin of the DF as renewed faulting, rapid development of local topographic variations, syn-sedimentary deformation of late early Visean strata [cf. *McCann et al.*, 2003] and an intra-Visean thickening of beds [*Garkalenko et al.*, 1971] (Figure 1c). The DF was uplifted in the Early Permian, especially its southern margin. It is classically thought that the Donbas "fold and thrust belt" was formed during the Permian [*Popov*, 1936, 1939, 1963; *Pogrebitsky*, 1937; *Stepanov*, 1937; *Gavrish*, 1989] in response to stresses related to the Uralian-Caucasian Variscan orogeny [*Milanovsky*, 1992]. In this framework, *Korchemagin and Yemets* [1987] inferred from observations of slickensides a compressive paleostress field, with NNE-SSW compressional axis, which they considered to be related to Permian fold development (though they stipulated a low reliability for the absolute dating of this compressive stress field). However, recent studies have shown that fault deformation of this age is normal in style and that the uplift occurred under transtension-extension phase accompanying a post-rift reactivation [*Stovba and Stephenson*, 1999]. *Gavrish* [1985] and *Chekunov* [1994] argued that the Permian uplift could have been due to a mantle diapir. Synchronous Early Permian volcanic activity in the Scythian Platform (cf. Figure 1a for location) lend supporting evidence [*Alexandre et al.*, 2003]. The occurrence of Cimmerian tectonic compression is observed where

Mesozoic sediments exist [*Popov*, 1963; *Konashov*, 1980]; it is recorded through the offsets of Triassic beds along the northern thrust planes [*Popov*, 1963; *Sobornov*, 1995]. At the end of Cretaceous times, the DF displays inversion with development at this time of localized folds commonly associated with thrust development [*Stovba and Stephenson*, 1999; *Saintot et al.*, 2003]. Deformation of this age was recognized in earlier studies ("orogenic" phase according to *Popov* [1936, 1939]; *Stepanov* [1937]) but was thought to involve relatively minor reactivation of structures formed during the main fold belt forming events in the Late Palaeozoic. *Korchemagin and Yemets* [1987] determined a corresponding Alpine strike-slip stress field with a NNW compressional stress axis. Finally, a Paleocene orogenic phase is reported [*Popov*, 1936, 1939, 1963; *Stepanov*, 1937].

3. Paleostress Field Reconstruction in the Donbas Fold Belt

3.1. Method and Data: Using Paleostress Analyses to Constrain Tectonic Evolution

[14] The method is based on the kinematics of small-scale brittle structures collected in the field. The kinematic data are inverted to compute stress tensors as described in detail elsewhere [*Angelier*, 1990, 1994]; such paleostress field analyses have previously been applied in detail in various areas [e.g., *Angelier et al.*, 1985; *Sébrier et al.*, 1985; *Bergerat*, 1987; *Mercier et al.*, 1987, *Hippolyte and Sandulescu*, 1996].

[15] A similar study, based on inversion of brittle microtectonic objects, was possible in the DF because most of its exposed stratigraphic succession (with the exception of the Cenozoic) is dominated by lithologies (predominantly limestones and sandstones) that are competent for brittle deformation. About 3500 small-scale brittle tectonic data were observed in the DF at 135 sites, in Proterozoic, Devonian, Carboniferous, Permian and Mesozoic rocks. Fault slip data sets have allowed computation of 82 local stress tensors (with characteristics listed in tables corresponding to stress maps in subsequent sections). Stylolithic peak, diaclase and tension gash orientations, where available, have been used to determine the position of one of the principal stress axes. In places, conjugate systems of shear joints and of en echelon tension gashes also provided information about the attitude of the three principal stress axes. In total, the microtectonic data inversion has resulted in the reconstruction of 123 stress states.

[16] Local stress states are then considered according to the attitudes of stress axes in order to reconstruct successive paleostress fields under which brittle deformation occurred (only approximately since amplitudes of block rotations around vertical axis are unknown in the DF). The relative ages of local stress states in sites exhibiting polyphase stress histories was established using classical criteria such as successive striae on the same fault plane, crosscutting relationships between fractures, determination of pre- or post- folding stress states (assuming that one of the principal stress axis is vertical–parallel to lithostatic pressure–when faulting occurred), and the age of affected stratigraphic units.

[17] The measured local stress state may reflect a combination of effects related to development of major structures as well as to the prevailing regional (tectonic) paleostress field. The former can be considered as "internal" stresses (as in a fold limbs during fold formation, or also along strike-slip fault zones). They can differ from the regional stress field not only in terms of stress trajectories but also by stress regime. Accordingly, the reconstructed paleostress stress states are presented in subsequent sections in the framework of their respective structural settings.

3.2. Southwestern Margin of the Ukrainian Donbas (Figure 2)

[18] The southwestern margin of the DF (and more the Ukrainian shield and the Azof Massif) was strongly uplifted in Permian times and, consequently, the underlying Proterozoic crystalline rocks and the Devonian to Lower Carboniferous syn-rift succession is exposed, giving access to the earliest history of basin formation. The Devonian to Lower Carboniferous stratigraphic succession in this area is characterized by extrusive rocks and continental clastics with intercalated volcanoclastic units, followed by a thick carbonate platform sequence (Figure 1d). The characteristics of all local stress states are listed in Table 1.

3.2.1. Observed Paleostress Events

[19] The oldest paleostress state observed in rocks of the DF southwestern margin is a tensional stress field with σ_3 trending NNE-SSW, recorded at nine sites in the Azov Massif and in Devonian-Lower Carboniferous rocks from normal faults and a very dense network of tension gashes (Figure 2a). A block structure characterizes the area with sedimentary layers dipping 10°–20° northward or eastward. Tilting is related to normal movements along WNW-ESE trending faults such as the Yujni Fault [cf. *McCann et al.*, 2003]. The NE-SW trending major fault zones (Figure 2) can be interpreted as being related to fault block development on the rift margin during the initial rifting phase. At site 9, the stress tensor reveals a transtensional regime along a set of NW-SE to NNW-SSE trending faults (see stereoplot on Figure 2a). Nevertheless, the general extension axis of the stress field trends perpendicular to the main WNW-ESE rift-related faults (Vassiliev, Volnovakha or Yujni Faults, see Figure 2), which might therefore have acted as purely normal faults (i.e., without oblique movements). This paleostress state likely corresponds to the Late Devonian stretching phase that initiated rift basin formation and to its reactivation in the Visean. Tournaisian-early Visean rocks are affected by this event and syn-sedimentary normal faults have been found in a late early Visean unit with related thickening of beds (site 105).

[20] A paleostress state with a NW-SE trending compressional axis was identified at 11 sites (Figure 2b). Strike-slip as well as reverse faults developed under this stress field and many stylolitic peaks display the NW-SE σ_1 axis. At eight sites, the σ_1 axis strikes E-W (Figure 2b, bottom left corner). No relative chronology could be established between these two compressional trends. However, numer-

Table 1. Characteristics of Local Stress States Corresponding to the Stress Fields Presented on Figure 2[a]

Site Number/Localities	Age of Rocks and Lithologies	N	σ_1 Dir.	σ_1 Pl.	σ_2 Dir.	σ_2 Pl.	σ_3 Dir.	σ_3 Pl.	φ	α	% RUP	Q	Ch.	Comments
N-S to NE-SW Extension on Figure 2a														
9/South of Razdolnoe Vassilievka fault zone	Archean granite/ Devonian volcanic rocks	12	323	78	113	10	204	06	0.7	13	32	3	1	NW-SE trending dykes, tension gashes and joints
10/Dalniy Quarry	Tournaisian-Visean limestones													nearly E-W trending dykes and normal faults
11/Nikolaevka Village	Archean granites/ Devonian deposits	6	311	64	072	14	168	21	0.2	20	42	1	*	
39/Maf Khaya -Styla	volcanic series													syn-tilting normal faulting
41/Styla Lake	sandstones (Visean?)													WNW-ESE tension gashes
73/Dokuchaevsk	Visean limestones													E-W trending normal faults + NE-SW tension gashes
105/Dokuchaevsk Quarry	lower Visean cherts and limestones													WNW-ESE syn-sedimentary faulting
108/SW of Styla Lake	Devonian succession												*	E-W joints
109/Sukhaya Volnovakha	volcanic plug													E-W joints
Strike-Slip Regime on Figure 2b														
9/South of Razdolnoe	Archean granite/Devonian	16	342	03	224	83	073	06	0.3	9	26	3	2	
Vassilievka fault zone	volcanic rocks	5	320	14	052	10	176	73	0.3	14	42	1		
		7	273	08	079	81	183	02	0.3	12	32	2		
10/Dalniy Quarry	Tournaisian- Visean limestones	8	324	02	234	01	122	88	0.1	20	44	2		Stylolites and associated planes
11/Nikolaevka Village	Archean granites and Devonian deposits	10	337	21	201	62	074	18	0.7	14	35	3		
	(Nikolaevskaya suite)	8	127	07	270	81	037	05	0.4	9	36	2		
19/Novotroitskoe	Tournaisian limestones	7	275	02	181	60	006	29	0.4	8	16	1		
30/Karakouba quarry	Tournaisian limestones	8	171	04	050	82	261	07	0.6	10	27	2		conjugate sets of en echelon tension gashes and stylolites
30/Karakouba quarry	Tournaisian limestones	87	102	01	355	85	192	05	0.5	9	24	3		conjugate sets of en echelon tension gashes and stylolites
31/Razdolnoe	Dolginskaya suite- Famennian													Conjugate system of shear joints: E-W comp. axis
32/Razdolnoe	Antomtaramsky suite- Frasnian													Conjugate system of shear joints: E-W comp. axis
40/Yujni Quarry	Visean limestones	28	288	04	152	84	018	04	0.4	12	34	3		
		10	114	05	023	08	239	81	0.4	15	46	2		Associated stylolites
		4	158	03	249	10	53	79	0.6	4	9	1		Associated stylolites and tension gashes
41/Styla lake	Visean limestones													NW-SE dextral en echelon tension gashes
68/Zhogolevsky quarry	Tournaisian Visean limestones	12	130	11	331	78	221	04	0.8	6	16	2	1	associated tension gashes
		22	105	07	229	78	014	10	0.3	7	19	3		
69/Central quarry Komcomolskoe	Visean limestones	24	320	03	078	84	230	05	0.3	11	37	3	1	associated tension gashes
		4	139	03	047	27	234	63	0.8	6	28	1		associated stylolites and horizontal tension gashes
73/Dokuchaevsk	Visean limestones	5	300	07	160	80	031	06	0.5	4	33	1		associated tension gashes
105/Dokuchaevsk Quarry	Lower Visean Chert unit and limestones	10	310	00	091	89	220	00	0.4	8	36	3		associated NW-SE tension gashes
107/Novotroitskoe quarry	Lower Carbonif. limestones	7	272	19	09	19	140	62	0.9	11	25	2		NW-SE slip parallel bedding planes
108/SW of Styla Lake	Devonian volcanogenic succession													NW-SE joints
109/Sukhaya Volnovakha	Volcanic plug												*?	NW-SE joints
Compressive Regime on Figure 2c														
9/Razdolnoe Vassilievka	Archean granite/ Devonian volcanic rocks	6	223	17	124	27	341	58	0.3	15	42	1		
11/Nikolaevka Village	Archean granites and Devonian deposits	15	246	11	023	76	154	10	0.7	13	33	3		
38/Volnovakha- Styla	Devonian series and Granite	6	006	27	208	61	100	09	0.6	1	12	2		And joints in Devonian series

Table 1. (continued)

Site Number/Localities	Age of Rocks and Lithologies	N	σ_1 Dir.	σ_1 Pl.	σ_2 Dir.	σ_2 Pl.	σ_3 Dir.	σ_3 Pl.	φ	α	% RUP	Q	Ch.	Comments
41/Styla lake	Visean Limestones													NW-SE dextral en echelon tension gashes plus E-W striking stylolitic planes
68/Zhogolevsky quarry	Tournaisian Visean Limestones	7	078	14	344	15	210	69	0.5	6	21	2	2	ENE-WSW/NE-SW tension gashes plus ENE-WSW stylolites
		16	180	12	272	07	031	76	0.4	8	17	3		conjugate sets of en echelon tension gashes
69/Komcomolskoe	Visean limestones												2	NE-SW tension gashes
					Trace of E-W Extension									
9/Razdolnoe Vassilievka	Archean granite/Devonian volcanic rocks	11	339	62	167	28	076	03	0.7	16	38	3	1	
10/Dalniy Quarry	Tournaisian- Visean limestones													N-S trending tension gashes and dyke
31/Razdolnoe	Dolginskaya suite- Famennian													N-S striking fractures dipping 60° W

[a]N, number of fault slip data to compute the stress tensor (using inversion method "INVD") [*Angelier*, 1990]. Dir. and Pl., trends and plunges of principal stress axes in degrees; $\phi = (\sigma_2 - \sigma_3)/(\sigma_1 - \sigma_3)$; α, average angle between observed slip and computed shear, in degrees (acceptable with $\alpha <$ 22,5°). RUP, criterion of quality ranging from 0% (calculated shear stress parallel to actual striae with the same sense and maximum shear stress) to 200% (calculated shear stress maximum, parallel to actual striae but opposite in sense), acceptable results with RUP < 75%. Q, quality as 3, high quality; 2, reliable; 1, poor quality. Ch., chronology between local stress events (in polyphase sites); asterisk signifies a back-tilted stress event.

ical modeling has shown that a NW-SE orientated maximum stress acting on the southern Donbas margin could be deviated into an E-W direction due to right-lateral strike-slip movement along the WNW-ESE trending fault zones (i.e., the Vassiliev and Yujni faults, Figure2b [cf. *Brem*, 2000; *Saintot et al.*, 2003]).

[21] A clearly younger stress field was inferred at 6 sites as a strike-slip regime with an average NE-SW trending σ_1 (Figure 2c). At two sites, reverse faulting occurred. These stress states are related to the development of large thrusts; the deviation of the σ_1 stress axis orientation at site 68 (From NNE to N) in Lower Carboniferous limestones is due to irregularities in mass displacements along such a major thrust plane, indicated by irregular trends of calcite steps.

[22] Along the Vassiliev and Yujni faults, an E-W extensional event was recorded by normal faulting and tension gashes at three sites (Figure 2d). These are inferred to be localized accommodation structures related to movement in the fault zones, rather than being indicative of a regional stress field.

3.2.2. Chronology and Summary of Paleostress Stress Trends on the Donbas Southwestern Margin (Figure 3)

[23] The succession of paleostress fields described above was established from field observations as follows. At site 9, successive grooves developed on the same fault plane: the first under a NNE-SSW extension and the second under a strike-slip regime with NW-SE trending σ_1 axis. At site 11, the attitude of normal faults is clearly pre-tilting whereas all other recorded stress events are post-tilting. At site 68, reverse faults that developed under the NE-SW compression crosscut tear faults that developed under the strike-slip regime with NW-SE σ_1 axis. At site 69, NE-SW directed tension gashes cut across the strike-slip fault planes related to the strike-slip paleostress regime with NW-SE trending σ_1 axis. At site 108, one set of tension gashes developed before tilting under the NNE-SSW extensional trend.

[24] Thus, two stress fields are well recorded on the southwestern DF margin and they undoubtedly both represent important tectonic events. The first is the extensional stress field affecting rocks of Devonian to early Visean age (in particular, the competent Tournaisian-early Visean limestones) and presumably related to intracratonic rifting during which the DDB initially developed. The second major tectonic phase is characterized by a strike-slip paleostress field with a NW-SE trending compressional axis (deviated to E-W between active fault zones). Strike-slip faults as well as reverse faults developed, suggesting that the paleostress field was a transpressive one.

3.3. Russian (Eastern) Part of the Donbas (Figure 4)

[25] In the easternmost, Russian part of the DF, the Main Anticline structure attenuates somewhat, with limbs dipping 45°–60°. The Konstantinovsky Fault zone lies along its hinge and is a right-lateral strike-slip fault according to associated fault patterns at its western termination (NNE-SSW striking normal fault pattern north of its trace and E-W striking reverse fault pattern south of it; Figures 4b and 4d). The northern and southern margins are respectively characterized by northward directed thrusts (the Almazny Fault zone) and southward directed thrusts (the Persianovsky Fault zone [*Pogrebnov et al.*, 1985]; Figure 4).

[26] Kinematic observations of brittle structures have been made in Carboniferous rocks as well as Cretaceous rocks (sites 20, 61, 65). Analysis of 900 brittle structures (including many tension gash sets) has allowed the infer-

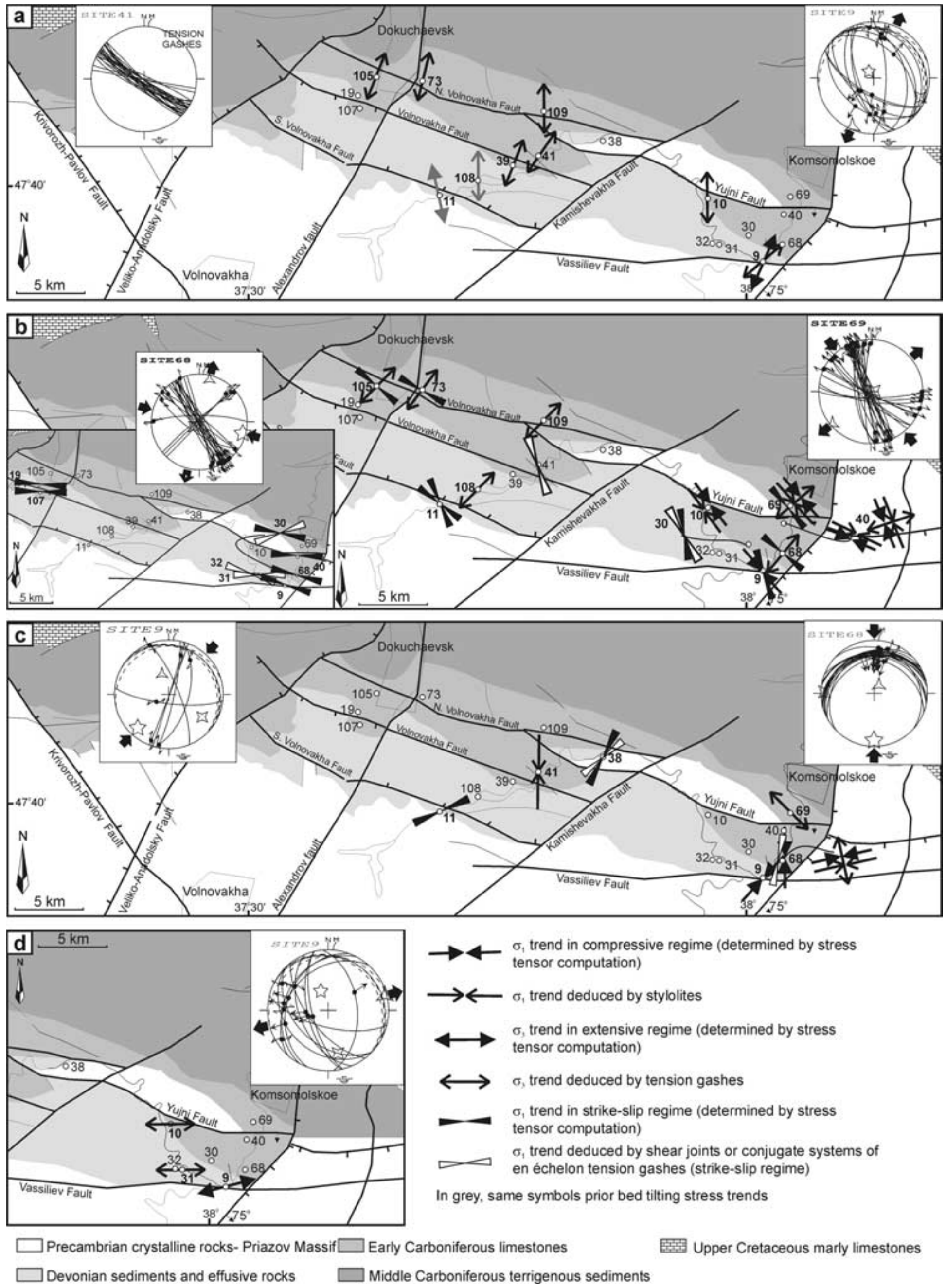

Figure 2. Paleostress field succession in the southwestern zone of the Donbas fold belt recorded in Proterozoic crystalline rocks, Devonian and Early Carboniferous volcanic and sedimentary succession. (a) Extensional stress trends relative to the rifting event. (b) A strike-slip and compressive regime with NW-SE trending σ_1 and E-W σ_1 stress axis deviation. (c) Compressional and strike-slip regime with NE-SW trending σ_1. (d) Some E-W directed tensional stress axis trends along the E-W striking major fault zones. Key for stereoplots: Schnmidt's projection, lower hemisphere; bedding planes as broken lines, fault planes as thin lines, striae as small arrows (inward directed = reverse, outward directed = normal, couple of thin arrows = strike-slip); computed stress axes as 5-, 4- and 3- branch stars (σ_1, σ_2 and σ_3, respectively); direction of compression: inward directed large arrows, direction of extension: outward directed large arrows. As background: extract of geological map of the Ukrainian Donbas fold belt [*Donetsk State Regional Geological Survey*, 1995].

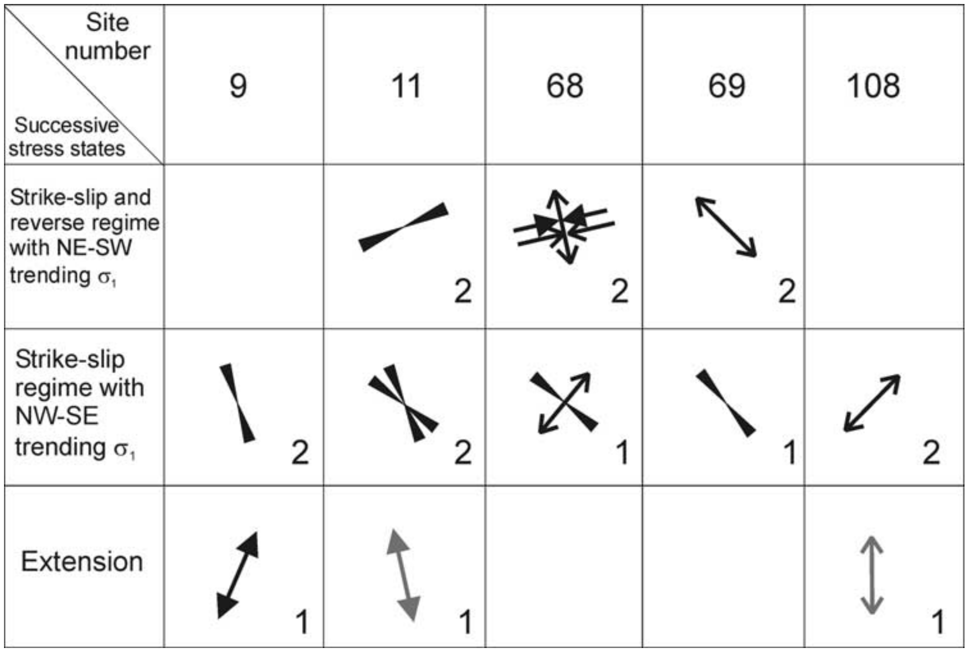

Figure 3. Chronology between local stress states in the southwestern margin of the Donbas (corresponding to paleostress field succession on Figure 2). Caption for stress axis trends (arrows and triangles) as for Figure 2.

ence of four successive paleostress fields based on differing directional trend, described below from the oldest to the youngest tectonic events. The characteristics of all local stress states are listed in Table 2.

3.3.1. Observed Paleostress Events

[27] Numerous tension gashes have been developed at 4 sites in Middle and Upper Carboniferous rocks under a stress regime with a NW-SE trending σ_3 axis (Figure 4a). At site 67, a set of NE-SW orientated tension gashes is also related to right-lateral strike-slip movement along a NNE-SSW to N-S striking main fault zone (cf. stereoplot Figure 4a; NE-SW trending stylolites and associated planes are also observed near the fault).

[28] Inversion of tension gashes and strike-slip faults measured in Middle and Upper Carboniferous sediments at six sites gives a strike-slip regime characterized by a N-S trending σ_3 axis (Figure 4b).

[29] Six sites have recorded, through the development of strike-slip fault systems and related tension gashes, the occurrence of a strike-slip regime with a NE-SW trending σ_3 axis (Figure 4c). This paleostress event affected Middle and Upper Carboniferous strata.

[30] The most unambiguously recorded paleostress field was seen at 17 sites and is characterized by a N-S to NE-SW trending σ_1 axis (Figure 4d). Reverse faults as well as strike-slip faults developed under this regime. The strike-slip stress field is also indicated by the synchronous development of N-S trending tension gashes and N-S striking stylolitic peaks (as at sites 51, 59 and 64). In contrast to the three older inferred paleostress fields, this stress event also affected Upper Cretaceous rocks (sites 61, 65).

3.3.2. Chronology and Structural Importance of the Reconstructed Paleostress Stress Trends in the Russian Donbas (Figure 5)

[31] The relative ages of local stress states, therefore between paleostress fields, is summarized in Figure 5. Pre- and post-tilting events were recognized at sites 50 and 51. Other relative ages were inferred from crosscutting relationships between brittle structures and successive striae on the same fault mirror. Therefore, from one site to another, it was possible to give a well-constrained chronology between the determined stress fields as presented in the previous paragraphs, except between the two intermediate stress fields (the strike-slip regimes with NE-SW σ_3 and with N-S σ_3).

[32] The youngest identified stress event occurred after Late Cretaceous times whereas the three others evidently occurred prior to the Late Cretaceous times but after the Late Carboniferous. Moreover, the three older events (Figures 4a, 4b, and 4c) mainly developed tensional features in contrast to the youngest (Figure 4d) that developed compressive structures such as reverse fault systems.

[33] Significantly, the last stress event is fully compatible with fold trends observed in the area. The trend of the shortening axis responsible for the fold development is systematically parallel to the maximum principal reconstructed stress axis trend. For instance, at several sites, the σ_1 stress axis has been found to be parallel to the dip direction of the tilted bedding planes. At site 65, in Upper Cretaceous chalks, the reconstructed N-S trending σ_1 stress axis is perpendicular to the spectacular localized close anticline axis (that could correspond to an anticline formed above a thrust plane). Moreover, at site 50, strike-slip stress

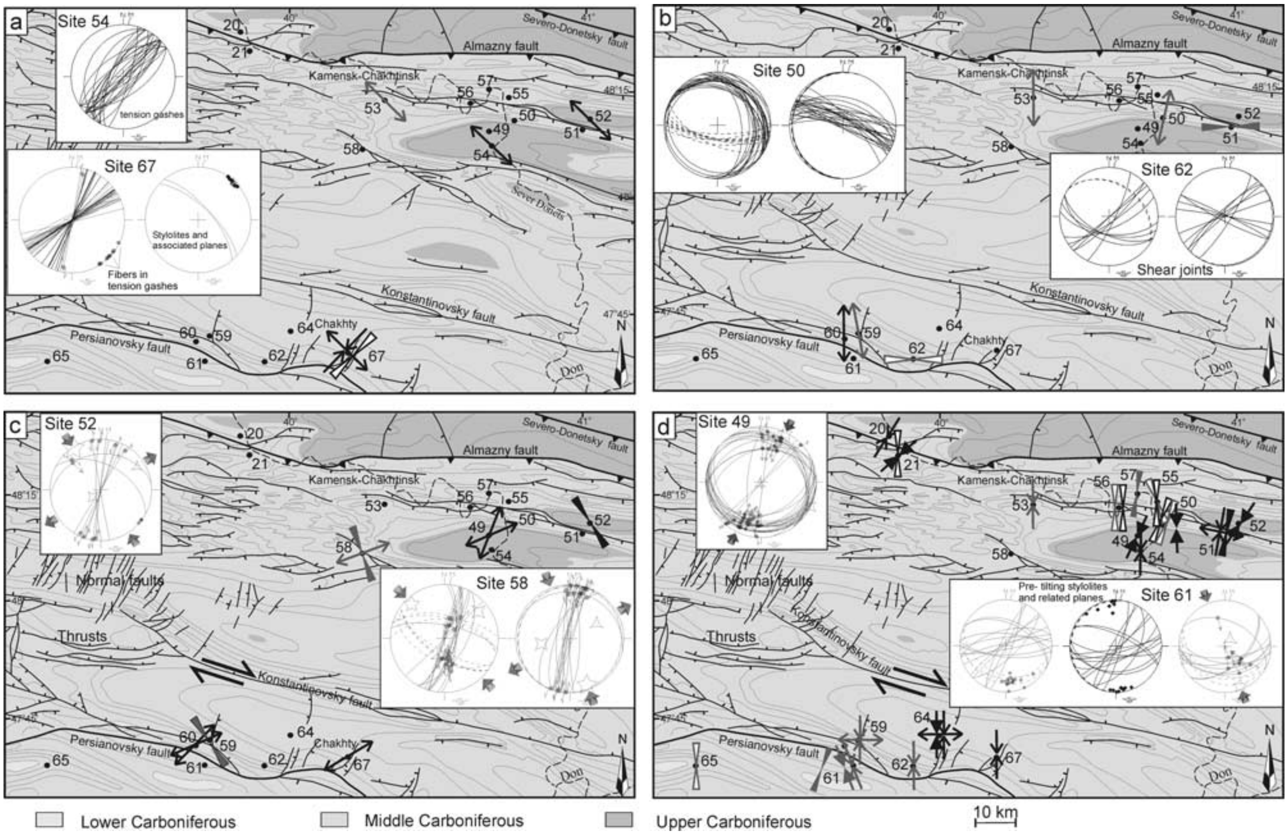

Figure 4. Paleostress field succession in the eastern ending of the Donbas recorded in Carboniferous and Upper Cretaceous strata. (a) NW-SE trending σ_3 axis in a strike-slip regime. (b) A strike-slip regime with a N-S trending σ_3 axis. (c) A strike-slip regime with a NE-SW trending σ_3 axis. (d) Compressional regime with N-S to NE-SW trending σ_1 axis. Caption for stress axis trends (arrows and triangles) and keys for stereoplots as for Figure 2. As background: Extract of geological and structural map of the Donbas [*Pogrebnov et al.*, 1985].

states occurred before and after the tilting of bedding planes and were followed immediately by a purely compressional stress event.

[34] Accordingly, it is inferred that the youngest stress event is responsible for the inversion of initially normal faults and that it formed the compressive structures (such as localized folds and associated thrust planes) at a time no older than the end of the Late Cretaceous.

[35] A final remark concerns the right-lateral strike-slip movement that occurred along the Konstantinovsky Fault (as indicated by the observed associated fault pattern described above). Two of the inferred paleostress fields could have generated the observed displacement and structural pattern, given their principal stress axes orientations relative to the fault orientation: the strike-slip regime with a NE-SW trending σ_3 axis (Figure 4c) and the N-S to NE-SW compressional regime (Figure 4d). These are the two best documented paleostress fields in terms of the measured number of related brittle structures and the number of affected sites. No major structures seem to have been developed under the effects of the two other inferred paleostress fields (NW-SE trending σ_3 axis, Figure 4a; N-S trending σ_3 axis, Figure 4b). These two stress fields are likely indicative of relatively minor tectonic events, leading only to the reactivation of inherited major fault zones.

3.4. Northern Zone of the Ukrainian Donbas (Figure 6): Record of a N-S to NW-SE Compression as the Youngest Tectonic Event

[36] The northern zone of the Ukrainian DF corresponds to the inverted northern margin of the initial rift basin. The traces of the NW-SE striking major fault zones in this area (Severo-Donestky, Marievsky and Almazny faults) present a lenticular shape (Figure 6). The area is characterized by localized close folds developed upon shallow thrust planes. The inversion of the northern margin has affected Upper Cretaceous strata.

[37] Most observations were of brittle structures in Carboniferous rocks but measurements were also taken from Permian (site 91) and Cretaceous aged strata (site 95). The 13 reconstructed local stress states (listed in Table 3) can be grouped to form one stress field (Figure 6) related to folding and thrusting processes along the northern margin of the basin. For instance, at seven sites (sites 86, 96, 97, 103, 120,

Table 2. Characteristics of Local Stress States Corresponding to the Stress Fields Presented on Figure 4[a]

Site Number/Localities	Age of Rocks and Lithologies	N	σ_1 Dir.	σ_1 Pl.	σ_2 Dir.	σ_2 Pl.	σ_3 Dir.	σ_3 Pl.	φ	α	% RUP	Q	Ch.	Comments
Strike-slip Regime With NW-SE Extensional Trend as on Figure 4a														
52/Zhirnovsky quarry	Upper Carboniferous limestones												1	NE-SW striking tension gashes
53/Repniensky quarry	Lower Moscovian sandstones												*	NE-SW tension gashes
54/Bogatov area	Upper Moscovian limestones												1	NE-SW tension gashes
67/Chakhtiy	Bashkirian-Moscovian sandstones												1	right-lateral strike-slip faults and associated stylolites and tension gashes
Strike-Slip Regime With a N-S Extensional Trend as on Figure 4b														
50/Belaya Kalitva	Upper Carb. sandstones limestones												*	E-W striking tension gashes
51/Zhirnovsky quarry	Upper Carboniferous limestones	8	269	05	023	78	178	11	0.4	6	21	2	*	
53/Repniensky quarry	Lower Moscovian sandstones												*	E-W tension gashes
59/Radionovska quarry	Bashkirian sandstones												1*	E-W tension gashes
60/Boldarevka	Bashkirian sandstones													tension gashes trending N090
62/Alekseevka	Bashkirian Sandstones												*	shear joints developed in strike-slip event with E-W comp.axis
NE-SW Extensional Trend in Strike-Slip Regime as on Figure 4c														
49/Belaya Kalitva	Upper Carboniferous limestones												1	NNW-SSE and WNW-ESE tension gashes
52/Zhirnovsky quarry	Upper Carboniferous limestones	10	327	02	229	73	058	17	0.1	6	27	2	2	
58/Likhaya	Moscovian limestones sandstones	15	160	10	260	46	061	43	0.3	8	30	3	*	associated tension gashes
59/Radionovska quarry	Bashkirian sandstones	11	146	06	053	26	247	63	0.3	12	34	3	*	
60/Boldarevka	Bashkirian sandstones													tension gashes trending N120 to N150
67/Chakhtiy	Bashkirian-Moscovian sandstones												2	NNW-SSE to NW-SE tension gashes and fibers
N-S to NE-SW Compression as on Figure 4d														
20/Podgornoe	Maastrichtian marls													reverse fault planes: trace of NE-SW compression
21/East of Lugansk- Podgornoe	Moscovian shales	5	359	18	244	53	101	32	0.2	13	30	1		associated jointing
21/East of Lugansk- Podgornoe	Moscovian shales	9	049	05	318	10	165	79	0.3	16	37	2		
49/Belaya Kalitva	Upper Carboniferous limestones	37	026	03	116	00	207	87	0.3	10	43	3	2	associated tension gashes
50/Belaya Kalitva	Upper Carboniferous sandstones													pre- and post tilting left lateral strike-slip faults in NNE-SSW comp
50/Belaya Kalitva	Upper Carboniferous limestones	8	179	13	084	20	301	66	0.5	8	30	2		
51/Zhirnovsky quarry	Upper Carboniferous limestones	7	191	21	041	66	285	11	0.3	10	44	2		associated tension gashes and stylolites
52/Zhirnovsky quarry	Upper Carboniferous limestones	24	214	02	123	07	322	83	0.5	8	29	3		
53/Repniensky quarry	Lower Moscovian sandstones												*	stylolites and reverse slips parrallel bedding planes: N-S compression
54/Bogatov area	Upper Moscovian limestones												2	N-S striking stylolites
55/Potselyevka quarry	Moscovian limestones sandstones												*	left-lateral strike-lip faults and tension gashes: NNW-SSE comp. axis;
55/Potselyevka quarry	Moscovian limestones sandstones													pre-tilting stylolites, shear joints and post tilting stylolites: N-S comp. axis
56/Belaya Kalitva	Upper Moscovian limestones													tension gashes and stylolites: N-S comp. axis
57/Potseloviev	Upper Moscovian sandstones	9	008	03	261	79	098	10	0.4	3	8	2	*	

Table 2. (continued)

Site Number/Localities	Age of Rocks and Lithologies	N	σ_1 Dir.	σ_1 Pl.	σ_2 Dir.	σ_2 Pl.	σ_3 Dir.	σ_3 Pl.	φ	α	% RUP	Q	Ch.	Comments
59/Radionovska quarry	Bashkirian sandstones												2*	N-S stylolites and associated planes and N-S tension gashes
61/Darievsky quarry	Turonian marly limestones	5	201	26	075	50	306	28	0.4	7	26	1	*	
61/Darievsky quarry	Turonian marly limestones												*	stylolites and associated planes: NNW-SSE comp
61/Darievsky quarry	Turonian marly limestones	9	159	09	251	13	036	75	0.6	9	21	3		
62/Alekseevka	Bashkirian Sandstones												*	N-S striking stylolites and associated planes
64/Chakhtiy	Bashkirian-Moscovian sandstones	6	360	10	261	43	100	45	0.2	8	24	2		associated stylolites and related planes and NE-SW striking tension gashes with oblique E-W fibers
65/Lisogorka	Cenomanian chalks												*	left-lateral strike-slip faults, tension gashes, stylolites: N-S comp.axis
67/Chakhtiy	Bashkirian-Moscovian sandstones													Isolated reverse faults, stylolites and associated planes: N-S comp. axis

[a]Definitions, abbreviations, and sources as for Table 1.

129, 130), the maximum principal stress axis (i.e., the pressure axis) is parallel to the direction of shortening.

[38] It is interesting to note that a deviation of the principal stress axis trajectory occurred in this area. Close to the NW-SE trending northern limit of the basin (Figure 6), σ_1 trends N-S whereas inside the basin, it trends NW-SE. Moreover, toward the center of the basin, the strike of the thrust planes becomes perpendicular to the σ_1 axis (sites 86, 120). The thrust planes were reformed under this NW-SE compression. The stress trends highlight the right-lateral movement that occurred along the northern margin during its inversion, also producing the lenticular shape of the traces of the fault pattern.

[39] It also suggests that stress trends recorded within the sedimentary basin are different than the regional stress trends (at the plate tectonic scale). Such a phenomenon could be explained by a rheological contrast between the crystalline host and sedimentary infill of the basin. In the present case, a N-S compressive trend could have been the trace of the regional trend. At polyphase site 120, a pre-tilting strike-slip stress tensor was inferred. It could be the legacy of the N-S compressive stress field that affected the basin just prior to folding and thrusting (that occurred under NW-SE directed compression in this zone). Alternatively, the right-lateral reverse movement along the northern major boundary faults may have produced the deviation of stresses with "secondary" thrust planes newly forming inside the basin (such as the Nikanorovsky Fault, between sites 86 and 120 on Figure 6). A deviation of σ_1 stress axis trajectory along the Almazny Fault zone, from sites 91, 129 and 101 to sites 127 and 121 (Figure 6), is also noted: the trajectory is N-S north of the Almazny fault and E-W to the south.

3.5. Paleostress Trends in the Main Anticline Zone of the Donbas (Figure 7)

[40] The records of three different stress fields have been recognized in the vicinity of the MA of the DF. The characteristics of all local stress states are listed in Table 4.

3.5.1. Observed Paleostress Events

[41] The oldest inferred stress field corresponds to the one directly related to the active development of the MA (Figure 7a). Brittle structures observed at 12 sites are clearly associated with the anticline development (Figure 8). They include sets of tension gashes (perpendicular to the bedding planes with trends parallel to the fold axis - sites 80, 81, 115, 110, 111 - and perpendicular to the fold axis - sites 115, 119), conjugate systems of strike-slip faults, and shear joints developed on the limbs of the MA (sites 87, 134).

[42] The second paleostress field that has been recognized on the MA is well documented at 6 sites (Figure 7b) and corresponds to the regional tectonic event affecting Upper Cretaceous strata in the DF (as well illustrated on Figure 6). Under this action of this NW-SE compression, the MA fault zones (located at the hinge of the anticline) acted as right-lateral strike-slip faults (Figure 7b).

[43] The last event is poorly recorded (at 4 sites along the MA; Figure 7c) and indicates a strike-slip structural regime with an E-W trending σ_1 axis. Any tectonic interpretation

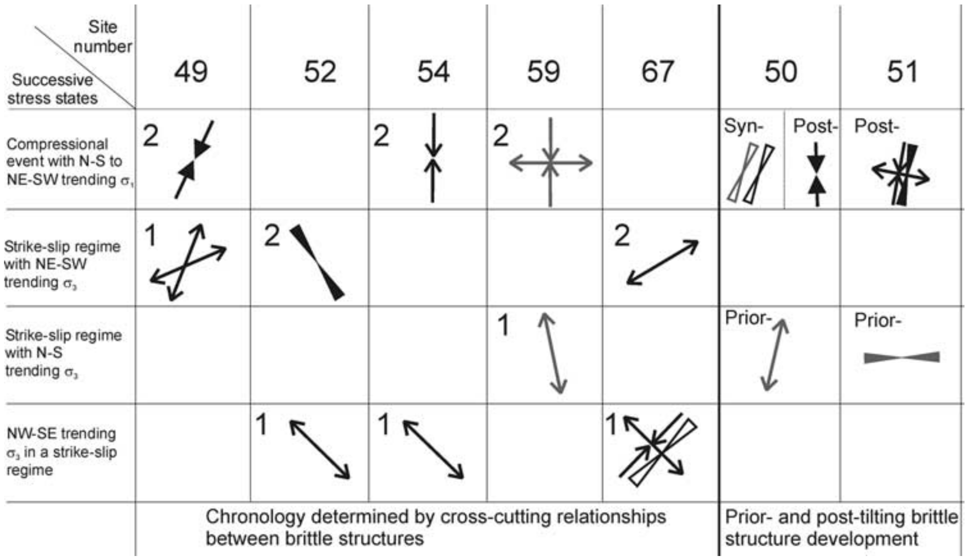

Figure 5. Chronology between local stress states in the eastern ending of the Donbas (corresponding to paleostress field succession in Figure 4). Caption for stress axis trends (arrows and triangles) as for Figure 2.

of this event is very speculative. However, such stress trends could be related to specific structures such as brachyanticlines that developed locally along the MA (e.g., site 87). Elsewhere (specifically, in the DF-DDB transition zone northwest of the MA), brachyanticlines can be seen to have developed as a result of salt tectonics that deformed the sedimentary succession up to and including Upper Cretaceous strata [*Balukhovsky*, 1959a, 1959b; *Popov*, 1963]. Paleostress indicators observed in this area (Figure 9) include a conjugate system of shear joints in Upper Cretaceous chalks (sites 24 and 25) and in Permian strata (site 26) as well as a very dense network of N20–N30 striking vertical joints (10–15 cm space interval) in an Upper Cretaceous chalk quarry at site 117. These brittle structures developed during active salt anticline growth during the Eo-Alpine tectonic period [*Stovba and Stephenson*, 1999]. It follows that similar structures related to the poorly recorded last stress event in the MA may have formed analogously.

3.5.2. Chronology Between the Stress Fields in the Main Anticline Zone

[44] At site 87, the relative ages of the first (formation of the MA; Figure 7a) and third mentioned paleostress fields (Figure 7c) is clearly demonstrated. The younger stress field (strike-slip regime with an E-W trending σ_1 axis) is clearly present both pre- and post-development of a local

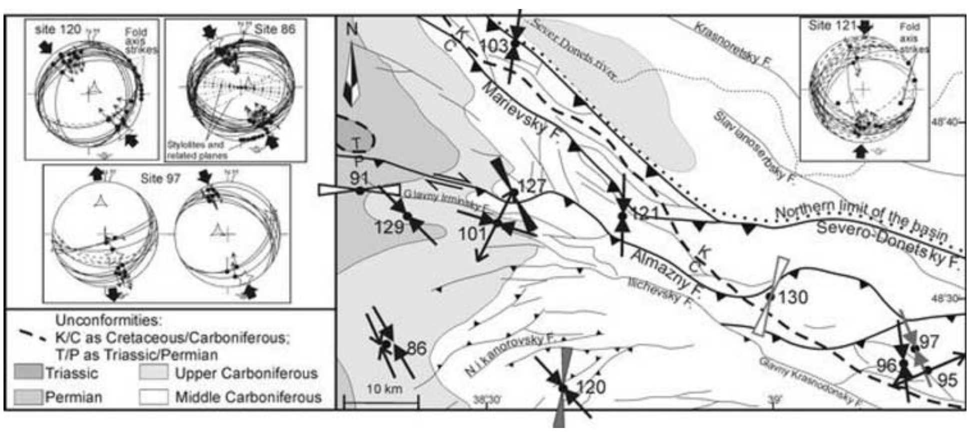

Figure 6. Paleostress trends in the northern zone of the Donbas: the record of a N-S to NW-SE compression as the last tectonic event. Caption for stress axis trends (arrows and triangles) and keys for stereoplots as for Figure 2. As background: Extract of geological and structural map of the Donbas [*Pogrebnov et al.*, 1985].

Table 3. Characteristics of Local Stress States Corresponding to the Stress Fields Presented on Figure 6[a]

			σ_1		σ_2		σ_3							
Site Number/Localities	Age of Rocks and Lithologies	N	Dir.	Pl.	Dir.	Pl.	Dir.	Pl.	ϕ	α	% RUP	Q	Ch.	Comments
86/Svetlodarsk	Upper Carb. limestones	32	331	02	240	12	072	78	0.4	9	31	3		associated stylolites and related planes
91/Artemovsk	Permian sandstones													shear joints as related to tilting
95/Georgievka	Campanian limestones													NNW-SSE joints
96/Lutugino	Middle Carboniferous	25	353	10	262	03	154	79	0.5	7	16	3		
97/Lutugino	Middle Carb. sandstones	9	159	10	067	12	287	74	0.5	7	29	3	*	
101/Pervomaisk	Upper Carb. limestones	11	108	35	238	43	357	27	0.5	15	37	2	*	associated tension gashes
103/Tochkovka	Moscovian sandstones	9	009	04	279	05	135	83	0.5	11	22	2		
120/Malo Ivanovka	Bashkirian limestones	4	006	19	243	58	105	25	0.6	4	26	1	*	
120/Malo Ivanovka	Bashkirian limestones	18	138	00	228	12	046	78	0.4	12	41	3		
121/Guardinski	Bashkirian - Moscovian sandstones	11	002	16	096	14	226	68	0.2	9	27	2		tilted fold axis in WSW-ENE trend
127/Pervomaisk	Upper Moscovian silts-sandtones	6	332	18	131	71	240	06	0.4	12	37	1		tilted fold axis in NE-SW trend
129/K. Popasnaya	Upper Carb. limestones	9	136	17	229	09	346	71	0.7	8	29	2		
130/Yurevka	Bashk. Mosc. sandstones													Strike-slip faulting related to folding

[a]Definitions, abbreviations, and sources as for Table 1.

Table 4. Characteristics of Local Stress States Corresponding to the Stress Fields Presented on Figure 7[a]

			σ_1		σ_2		σ_3							
Site Number/Localities	Age of Rocks and Lithologies	N	Dir.	Pl.	Dir.	Pl.	Dir.	Pl.	ϕ	α	% RUP	Q	Ch.	Comments
Strike-Slip Regime With WNW-ESE Trending σ_3 Related to the Main Anticline Growing														
5/Main anticline	Bashkirian sanstones													NNE-SSW trending tension gashes: σ_3' N110
6/Moguila Ostraya	Bashikirian sandstones													NNE-SSW trending tension gashes: σ_3' N110
78–79/Mius River	Moscovian Kasimovian sandstones													Nearly E-W striking joints (extrados)
78–79/Mius River	Moscovian Kasimovian sandstones													NNE-SSW trending tension gashes: σ_3' N110
80/Kirovskoe	Bashkirian sanstones													Jointing related to tilting
81/Olkhovatka	Bashkirian sanstones												*	Pre-tilting NE-SW joints
87/Nikitovka	Bashkirian sandstones	4	022	06	288	33	121	56	0.05	6	19	1	*	associated jointing related to tilting
110/Kamenka	Moscovian siltstones												*	N030 system of joints
111/Kamenka	Moscovian siltstones												*	N020 system of joints
115/Orlovo Ivanovka	Moscovian sandstones												*	N020-N030 system of joints
115/Orlovo Ivanovka	Moscovian sandstones													WNW-ESE joints (extrados)
119/Andreevka	Bashkirian sandstones													WNW-ESE trending tension gashes (extrados)
119/Andreevka	Bashkirian sandstones	4	209	04	118	05	339	84	0.6	9	30	1	4	
119/Andreevka	Bashkirian sandstones	6	090	73	190	03	281	16	0.7	6	26	2	6	
120/Malo Ivanovka	Bashkirian limestones	4	006	19	243	58	105	25	0.6	4	26	1	*	
134/Drujnoe	Moscovian sandstones												*	shear joints related to tilting
Strike-Slip Regime With NW-SE Trending σ_1														
75/Fachevka	Gzhelian sandstones	8	325	12	234	04	125	77	0.5	7	26	3		
76/Balka Fachevka	Moscovian- Kasimovian	5	296	08	199	44	034	45	0.1	5	33	1	*	
80/Kirovskoe	Bashkirian sanstones	7	331	02	218	85	061	05	0.6	4	11	2	*	
81/Olkhovatka	Bashkirian sanstones	24	338	19	210	61	076	21	0.4	12	36	2	*	
86/Svetlodarsk	Upper Carb. limestones	32	331	02	240	12	072	78	0.4	9	31	3		Associated stylolites and related planes
118/Konstantinovka	Lower Triassic sandy clays													NW-SE dip slip normal faulting
120/Malo Ivanovka	Bashkirian limestones	18	138	00	228	12	046	78	0.4	12	41	3		
Strike-Slip Regime With E-W Trending σ_1														
7/Main anticline	Bashkirian sandstones												*	Sets of NE-SW and E-W trending joints
78–79/Mius River	Mosc.- Kasim. sandstones	4	270	06	017	71	178	18	0.7	6	14	1		
87/Nikitovka	Bashkirian sandstones	5	109	05	218	76	018	13	0.5	4	17	2	*	
87/Nikitovka	Bashkirian sandstones	10	277	09	052	77	185	09	0.5	6	22	3		

[a]Definitions, abbreviations, and sources as for Table 1.

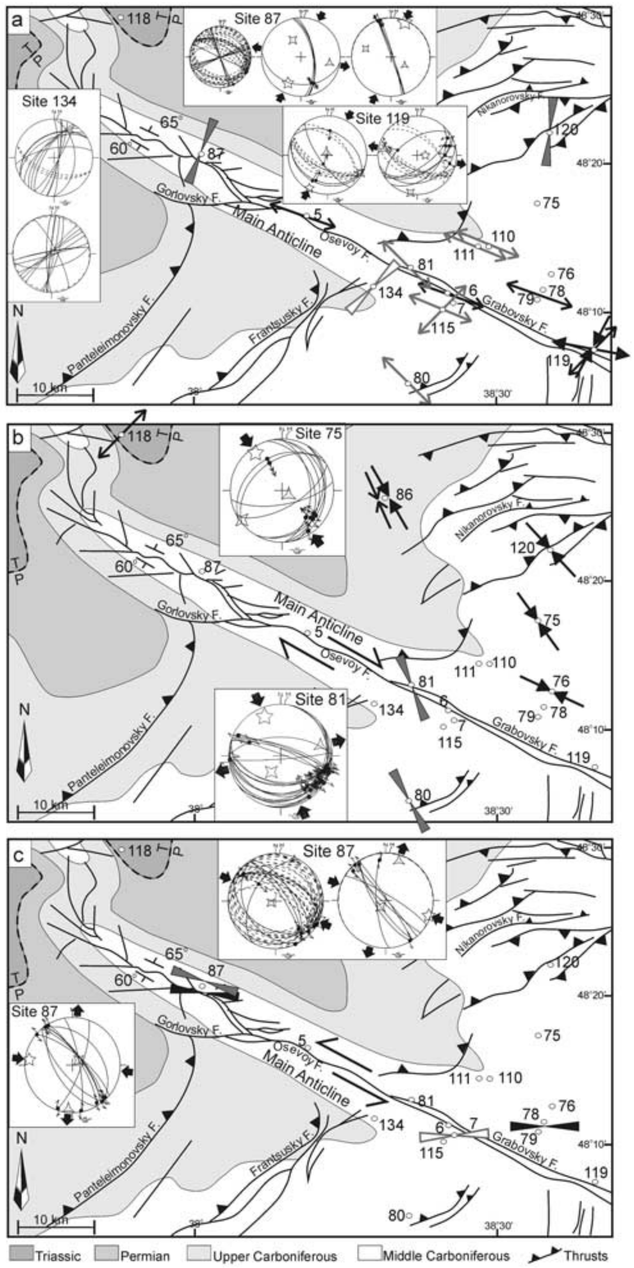

Figure 7. Paleostress field succession in the Main Anticline zone. (a) Stress axis trends related to growing of the Main Anticline. (b) Stress field corresponding to the latest tectonic event recorded in the Donbas: a NE-SW compression along the Main Anticline (cf. Figure 6). (c), Trace of a strike-slip regime with E-W trending σ_1. Caption for stress axis trends (arrows and triangles) and keys for stereoplots as for Figure 2. As background: Extract of geological and structural map of the Donbas [*Pogrebnov et al.*, 1985] (for relevant caption see Figure 6).

brachyanticline at this site (pre- and post-tilting stress tensors; see stereoplots on Figure 7c).

[45] At site 120 (presented on Figure 6), the pre-tilting stress tensor could correspond to the stress field related to MA formation (Figure 7a) with the post-tilting tensor belonging to the last compressional event (Figure 7b).

[46] No chronology exists between the NW-SE compression (Figure 7b) and the strike-slip field with the E-W pressure axis (Figure 7c).

3.6. Southern Zone of the Donbas (Figure 10)

[47] The southern zone of the DF is characterized by two gentle WNW-ESE folds (syncline and anticline). Twenty-five stress states (with characteristics listed in Table 5) were documented in this area, corresponding to three separate paleostress fields.

3.6.1. Observed Paleostress Events (Figure 10)

[48] The oldest paleostress field in this area is a strike-slip regime with an E-W trending σ_1 axis, constrained at five sites (Figure 10a). It affected (Serpukhovian and Bashkirian) Carboniferous rocks but not Upper Cretaceous cover. This stress field is unique and difficult to interpret because the trend of the maximum principal stress axis is nearly parallel to the trends of the general WNW-ESE structural grain of the area (fold axes and major fault zones–Mushketovsky and Prodolniy faults). Nevertheless, in this area, faults trending nearly N-S and dipping eastward (Meridionalny, Dulinsky, and Markovsky faults) or westward (Ilovaisky and Frantsusky faults) could have moved as reverse faults under such a stress field.

[49] Middle Carboniferous as well as Upper Cretaceous sediments both record a strike-slip regime with a NW-SE trending σ_1 axis (Figure 10b) at 10 sites. At sites 71 and 47, the local calculated stress tensors clearly show a transpressive regime with Φ ratio equal to 0.1. It is inferred that, under this stress field, the major WNW-ESE trending faults in this area were oblique thrusts and that the N-S trending faults were left-lateral strike-slip faults (as micro-faults at site 47, where both fault trends are present). In Upper Cretaceous strata, this paleostress regime clearly generated thrust planes at small as well as at large scales, accompanied by folding.

[50] At seven sites, a strike-slip to compressive paleostress regime with a nearly N-S trending σ_1 axis is indicated (Figure 10c). Thrusts (and, locally, folds) developed in Upper Cretaceous rocks under this stress regime, as under the previous one.

3.6.2. Chronology of Paleostress Fields in the Southern Zone of the Donbas

[51] The first strike-slip regime (with E-W σ_1; Figure 10a) is characterized by back-rotated local stress states at polyphase sites (15, 22, 28, 36), whereas the other stress states are post-tilting of bedding planes at the same sites (Figures 10b, 10c, and Table 5). Moreover, in this zone, this event affected only Carboniferous and not Upper Cretaceous rocks whereas the last two events both developed thrusts within Upper Cretaceous strata. At site 14, the NW-SE transpression occurred prior to the tilting of beds whereas the observed NNE-SSW compression occurred after tilting. Both regimes can, nevertheless, be considered as part of the same regional tectonic phase that

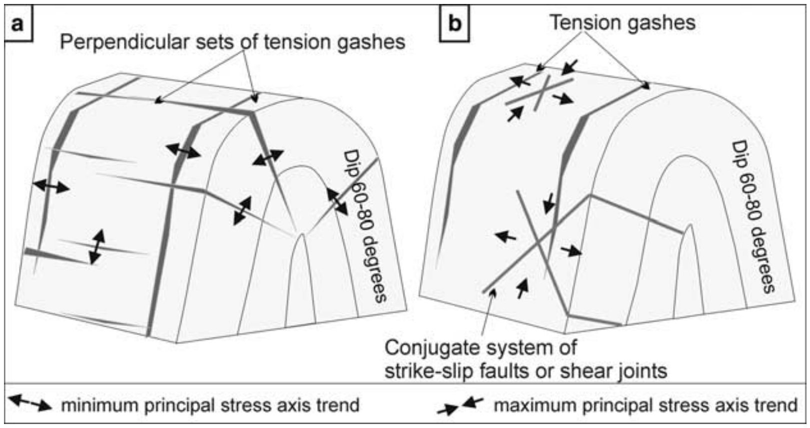

Figure 8. Brittle structures associated with the Main Anticline growing (stress trends illustrated on Figure 7a). (a) Perpendicular sets of tension gashes (as at site 115). (b) Tension gashes and conjugate systems of strike-slip faults or shear joints (as at sites 134).

produced thrusts and folds at the end of the Cretaceous in the DF.

4. Synthesis of Paleostress Analyses and New Constraints on the Structural Evolution of the Donbas Fold Belt

[52] The paleostress analyses for each of the separate zones of the DF can be extrapolated to determine the paleostress history of the DF as a whole. The main problem is to fix the absolute chronology of the various documented stress fields. The general lack of Triassic-Jurassic-Lower Cretaceous strata outcropping in the DF itself, means that a complete stratigraphic control on the timing of tectonic events is not possible. Nevertheless, several hypotheses concerning the stress history of the DF can be made based on the presented paleostress results and data from the published literature.

[53] Figure 11 (synthesis of the more detailed Figures 2, 4, 6, 7, 9, and 10) summarizes the successive paleostress fields that have been reconstructed in the various structural zones of the DF. In each zone, the relative chronology between the successive stress regimes has been established (section 3) with the exception of the two youngest events observed in the western MA zone (Figures 7b and 7c) and the two intermediate ones in the eastern part of the DF (Figures 4b and 4c). Figure 12 illustrates the trends of successive stress fields.

[54] The extensional stress field (Figure 11) inferred to be related to the initial rifting phase of basin development is only recorded on the southern DF margin where it is well-documented in exposed Devonian and Lower Carboniferous rocks (Figure 2a). Because the younger sedimentary succession was not affected by this event, there is little doubt concerning its relationship with the earliest tectonism of the basin development (e.g., intracratonic rifting). The minimum stress axis lies NNE-SSW perpendicular to the rift axis (as also inferred by *Korchemagin and Yemets* [1987]; Figure 12a). Under this NNE-SSW extension, the main WNW-ESE rift faults might have acted as purely normal faults whereas transtensional deformation could have occurred along the major NE-SW oblique faults of the southwestern margin of the DF (cf. Figure 2).

[55] The second stress regime, recognized in two zones, is a strike-slip regime with a NW-SE trending σ_3 axis

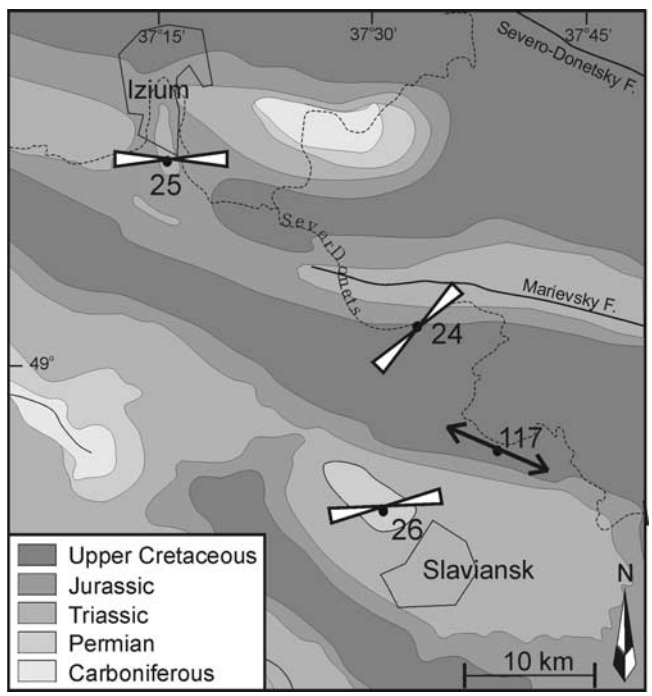

Figure 9. Paleostress states in the northwestern zone of the Donbas fold belt recorded in Permian and Upper Cretaceous series. Conjugate shear joints and single set of vertical joints are both related to brachyanticline growing. Caption for stress axis trends (arrows and triangles) as for Figure 2. As background: Extract of geological map of the Ukrainian Donbas fold belt [*Donetsk State Regional Geological Survey*, 1995].

Table 5. Characteristics of Local Stress States Corresponding to the Stress Fields Presented on Figure 10[a]

Site Number/Localities	Age of Rocks and Lithologies	N	σ_1 Dir.	σ_1 Pl.	σ_2 Dir.	σ_2 Pl.	σ_3 Dir.	σ_3 Pl.	ϕ	α	% RUP	Q	Ch.	Comments
Strike-Slip Regime With E-W Trending σ_1														
1/Amvrosevskaya	Bashkirian limestones	5	072	06	163	12	315	77	0.7	5	21	1	*	
15/Meridionalny fault	Serpukh.- Bash. sandstones	17	290	08	137	82	021	04	0.5	18	49	3	*	associated tension gashes
22/Blagodatnoe	Bashkirian limestones	4	259	01	161	81	350	09	0.5	3	12	1	*	associated tension gashes
28/Mospino	Bashkirian sandstones	12	068	07	251	83	158	00	0.6	11	35	3	*	
36/Blagodatnoe	Serpukh. siltstones	8	292	03	182	81	022	09	0.7	8	27	3	*	associated tension gashes
Compressional and Strike-Slip Regime With NNW-SSE Trending σ_1														
14/Amvrosevska	Upper Cret chalks	7	159	03	259	74	068	16	0.3	9	31	3	*	
15/Meridionalny fault	Serpukh.- Bash. sandstones	4	336	13	245	03	142	77	0.6	4	23	1		associated stylolites
27/Mospino	Bashkirian sandstones													conjugate system of shear joints
28/Mospino	Bashkirian sandstones	10	157	07	264	68	064	21	0.3	11	29	2	*	NNW-SSE trending associated tension gashes
28/Mospino	Bashkirian sandstones	13	159	08	251	11	032	76	0.5	7	19	3		syn-folding asociated stylolites
29/Mospino	Bashkirian sandstones													Isolated left-lateral strike-slip faults and shear joints
35/Oznovnoe quarry	Upper Cret. chalks	5	139	35	302	54	044	08	0.6	22	54	1		
42/Starabeshevo	Sepukh.siltstones													NW-SE tension gashes
46/Novopetrovskoe	Bashkirian												*	tension gashes, reverse faulting and stylolitic planes
47/Artemovka	Middle Bashkirian	7	348	14	103	58	250	27	0.1	9	29	2	*	
48/Licitche	Upper Cret. chalks	8	298	015	115	75	208	01	0.7	7	25	2	*	
71/Novi Svet	Serpukh. sandstones	7	330	05	061	09	214	79	0.1	7	31	2		
Compressional Regime With N-S to NE-SW Trending σ_1														
12/Donetsk	Bashkirian shales												*	folding and reverse parallel bedding slips
12/Donetsk	Bashkirian shales	6	005	02	273	35	098	54	0.6	11	28	2		
14/Amvrosevska	Upper Cret. Chalks	5	197	09	301	58	102	30	0.4	17	37	2		associated tension gashes
14/Amvrosevska	Upper Cret. Chalks	11	023	02	293	10	123	80	0.5	9	20	3		
16/Meridionalny fault	Serp.-Bash. sandstones													stylolites and associated planes
22/Blagodatnoe	Bashkirian limestones	19	208	06	299	11	090	77	0.5	17	46	3		tension gashes related to folding
36/Blagodatnoe	Serpukh. siltstones	6	164	17	071	09	314	70	.003	8	33	2		
48/Licitche	Upper Cret. chalks	14	043	05	300	69	135	20	0.3	8	30	3	*	
48/Licitche	Upper Cret. chalks	5	251	15	062	75	160	02	0.7	3	18	1		

[a]Definitions, abbreviations, and sources as for Table 1.

(Figures 11 and 12b). It has been argued that this regime is linked directly to growth of the MA (Figure 7a). But in the eastern part of the DF (Figure 4a), this stress event is more widely recognized and could be the legacy of a regional stress field. This event, in view of its age relative to the other stress regimes (it is the oldest one in the MA zone and in the eastern DF) and the age of the affected rocks, could correspond to an early Permian transtensional event recognized by *Stovba and Stephenson* [1999] in the nearby DDB. Its geometry fits with the development of WNW-ESE folds (such as the MA but also the open southern and northern synclines and anticlines; cf. Figures 1b and 1c) that have been formed in Permian times. The seismic data presented by *Stovba and Stephenson* [1999] showed that faults at this time have a normal component of displacement. No reverse faults (as micro-tectonic objects), thereby indicating a compressional stress component in this strike-slip regime, were found during the course of the present study. Given the inferred normal component of fault displacement and according to the reconstructed paleostress orientations, it follows that the Permian ‘‘folding’’ phase in the DF occurred in a transtensional stress regime with a NW-SE trending σ_3 axis. In such a case, salt tectonics could have controlled WNW-ESE trending anticline and syncline development (including especially the MA) in the DF, just as it has in the adjacent DDB [cf. *Stovba and Stephenson*, 1999, 2002; *Stovba et al.*, 2003; *Saintot et al.*, 2003]. Preliminary interpretation of new deep seismic reflection data across the MA (the first such data) indeed suggests the presence of a salt body deep in its core [*Roy-Chowdhury et al.*, 2001].

[56] The third set of paleostress states (Figures 11 and 12c) is formed by a group of observations that indicate strike-slip deformation with an E-W σ_1 trend that is difficult to correlate with the general structural grain of the DF. These stress records, although similar in character and seen in all of the structural zones of the DF, may not have been developed in a single, common stress regime. Locally, in the northwesternmost part of the DF (DDB transition zone; Figure 9) and along the MA (Figure 7c), the observed deformation could be related to the growth of brachyanticlines during post-Cretaceous salt movements (cf. section 3.5.1). On the southwestern margin of the DF, it could be due to local stress trajectory deviation within the regional Late Cretaceous tectonic stress regime with

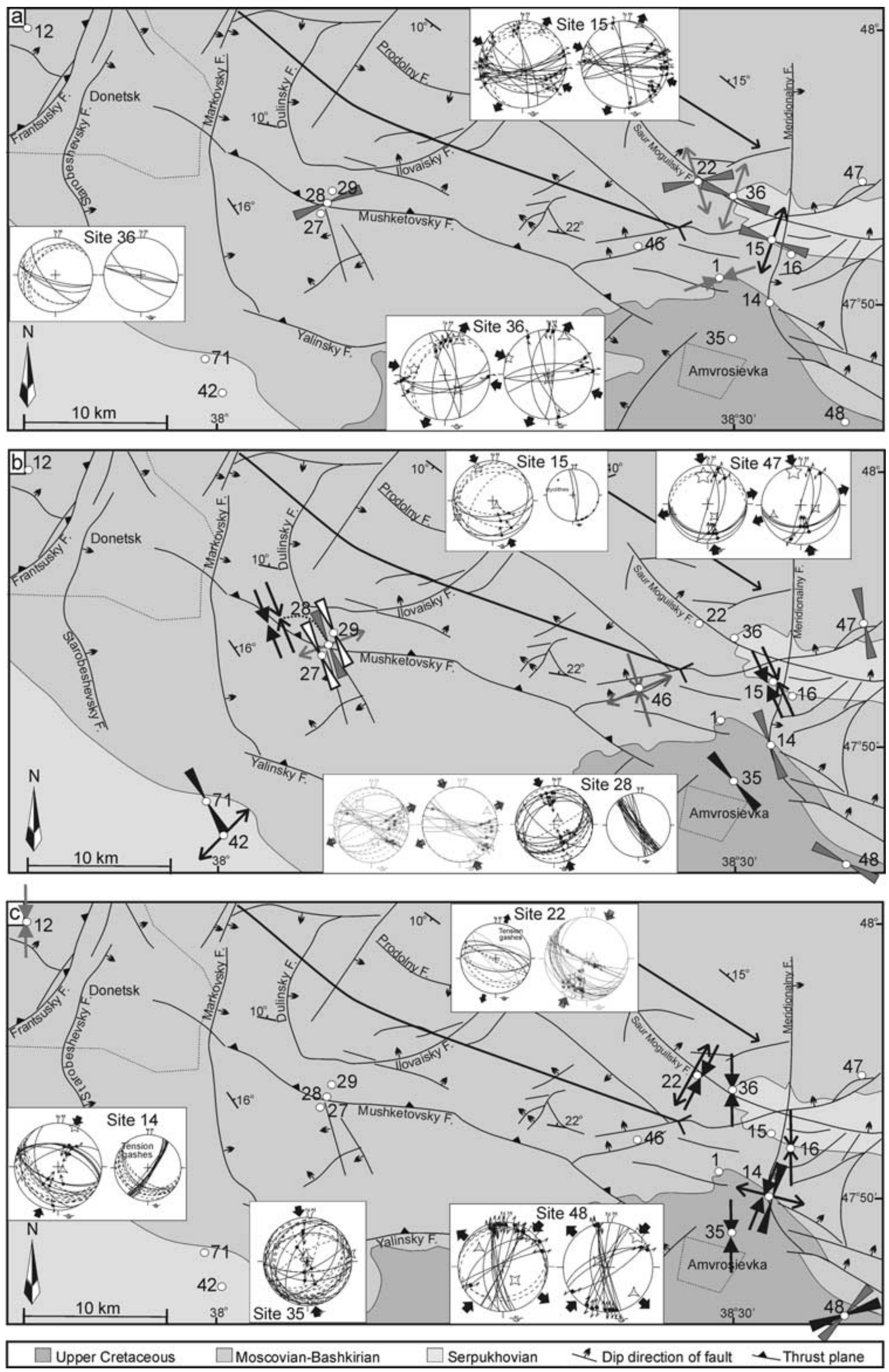

Figure 10. Paleostress states in the southern zone of the Donbas fold belt recorded in Carboniferous and Upper Cretaceous series. Caption for stress axis trends (arrows and triangles) and keys for stereoplots as for Figure 2. As background: Extract of geological map of the Ukrainian Donbas fold belt [*Donetsk State Regional Geological Survey*, 1995].

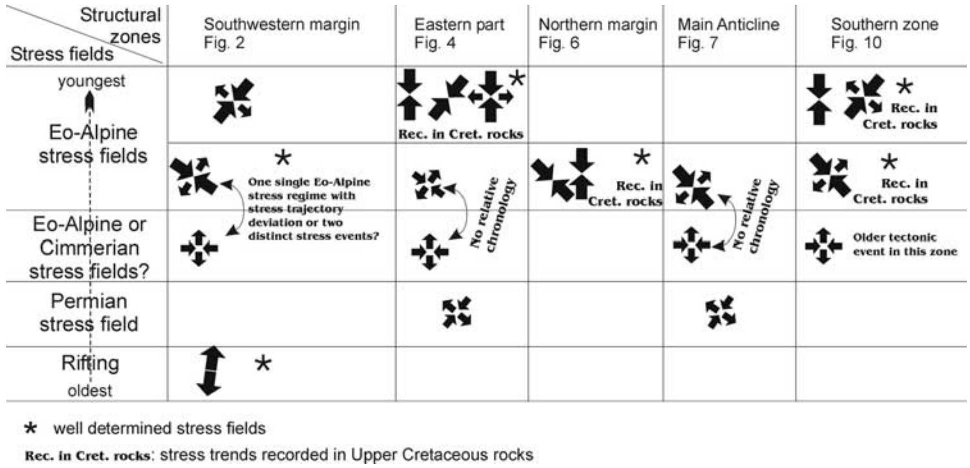

Figure 11. Synthesis on the succession of paleostress fields in the Donbas fold belt. Couple of convergent arrows: σ_1 trend; Couple of divergent arrows: σ_3 trend. In strike-slip regime, couple of large convergent arrows shows that compressive stress tensors are grouped in the strike-slip regime (i.e., under this regime strike-slip but also reverse faults developed).

NW-SE striking σ_1 (Figure 2b and cf. section 3.2.1). In the eastern (Figure 4b) and southern (Figure 10a) zones of the DF, however, there is evidence of a well-defined single stress field of more regional significance. This could be related to Triassic-Jurassic Cimmerian tectonics, including thrusting in the easternmost DF [*Popov*, 1963; *Konashov*, 1980; *Stovba and Stephenson*, 1999] and Karpinsky Swell [*Sobornov*, 1995]. Following, this stress field can be reconstructed using the observations of the eastern and southern zones (Figures 4b and 10a) and also, those of the southwestern and the MA zones (Figures 2b and 7c). In this scheme, E-W compressive trends would not correspond to an Eo-Alpine deviation of stresses in the southwestern zone and would not be related to brachyanticline formation in the MA zone. Such a strike-slip stress regime might have concentrated left-lateral deformation on the major WNW-ESE striking faults and generated transpressional deformation along the margins of the DF (including the reverse component of the well known thrusting of the Cimmerian deformation).

[57] The two youngest stress events (Figure 11) are well defined in the whole of the DF and both affected Upper Cretaceous rocks. They both display compressive as well as strike-slip stress tensors and are closely related to the last folding and thrusting stage that affected the DF. Associated anticlines are commonly developed above shallow thrust planes (e.g., site 28, in Cretaceous rocks at sites 14 and 35 on Figure 10b, at site 120 on Figure 7b, at site 68 on Figure 2c). These two stress fields clearly are reflecting Eo-Alpine tectonism in the DF. In detail, this tectonic phase can be characterized by two successive stress fields: a strike-slip-compressional regime with NW-SE trending σ_1 [cf. *Korchemagin and Yemets*, 1987] immediately followed by second strike-slip-compressional regime with N-S to NE-SW trending σ_1. Maps on Figures 12d and 12e show the orientations of the maximum stress axis corresponding to these two stress fields. The first of these Eo-Alpine stress fields is well documented in the MA zone and north of it (Figure 12d) but there is no evidence of the second event in either of these areas. In all other zones, both are well developed.

[58] The present study, taking into account all reconstructed paleostress trends and geometries of major structures, supports a new tectonic model for the evolution of the Donbas fold and thrust belt. Basin development began as a result of rifting during Late Devonian-Early Carboniferous times synchronous with that observed in the DDB to the northwest. The marginal faults of the DF acted as normal faults at that time. According to conventional views, the DF area, in particular its southern margin, was uplifted in the Permian. However, in significant contradiction to conventional models, the WNW-ESE trending "folds" of this age developed within a transtensional [?] stress regime that has not been strongly recorded in the DF as a whole. The occurrence of a Cimmerian tectonic phase not been unequivocally recorded in the DF although, the strike-slip stress field with an E-W compressional axis could be an indication of Cimmerian tectonics. A major Eo-Alpine (latest Cretaceous-Palaeocene) tectonic phase consists, in detail, of two successive strike-slip-compressional stress fields. Only one of them is recorded and developed significant structures in the northern zone and along the MA of the DF. This tectonic event is responsible for widespread thrusting and folding. Both events are otherwise widely documented throughout the DF. Right-lateral movement along the northern margin of the DF and the MA fault zones is well documented and is consistent with the geometry of the Eo-Alpine tectonic stress field.

5. Relationships of Paleostress Fields in the Donbas With Geodynamics Setting

[59] The observed DF paleostress orientations, and the tectonic events they signify, allow some geodynamic infer-

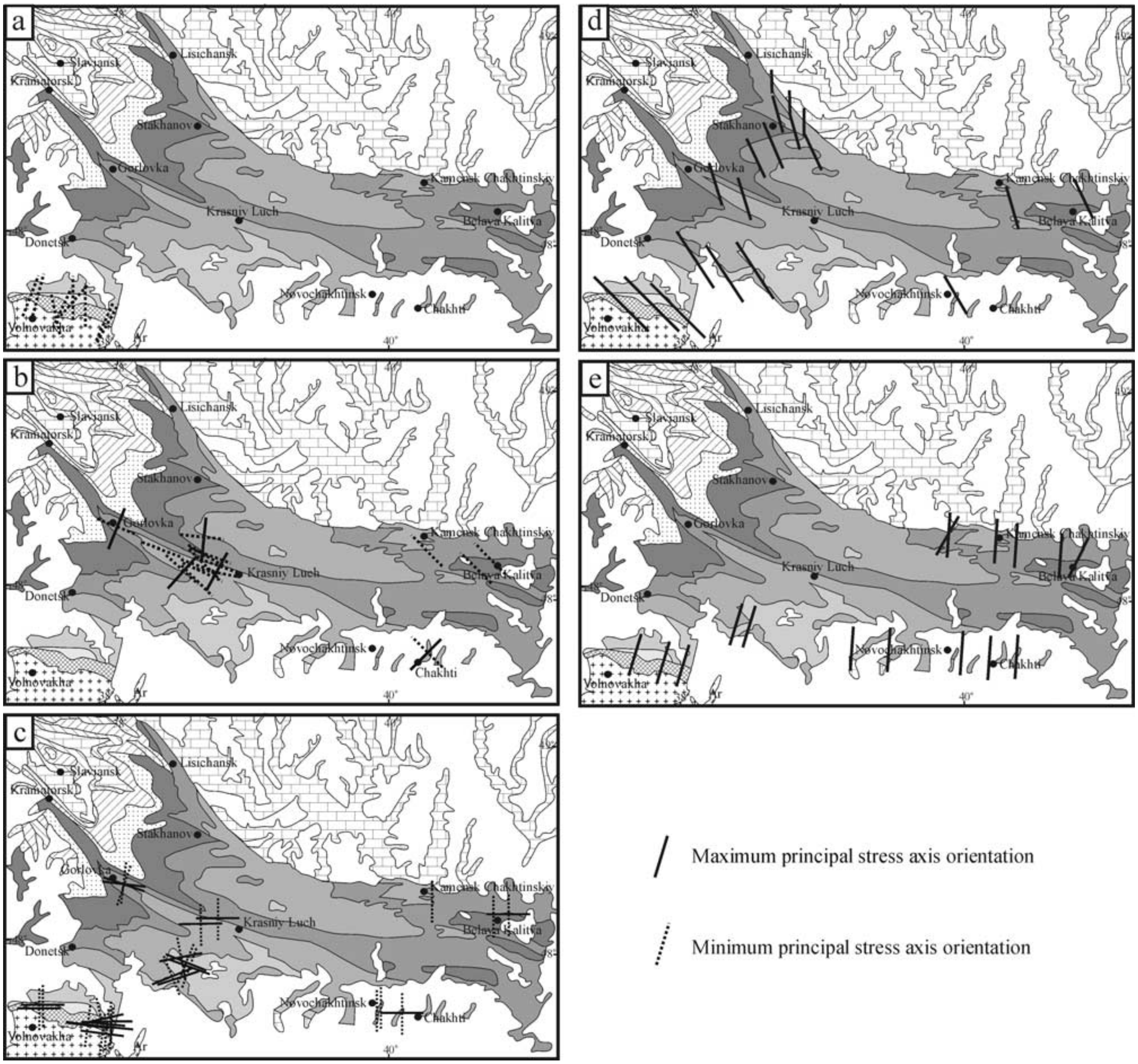

Figure 12. Maps of stress trends of the successive stress fields and of the density of records for each stress field. (a) The tensional stress states related to Devonian-Early Carboniferous rifting. (b) Record of the Early Permian stress field. (c) A strike-slip regime with transpressional deformation as record of the Cimmerian (?) tectonic event. (d and e) The two successive compressive stress fields affecting Upper Cretaceous rocks.

ences to be made about plate boundary processes affecting the southern part of the East European Craton (EEC) since the Late Palaeozoic. The DF, in this respect, lies in a key location as regards both Variscan/Uralian (Hercynian) and later Tethyan belt growth and evolution of the European continent.

[60] The Donbas belongs to a paleorift system that developed in the present-day southern EEC during Late Palaeozoic times that included the Dnieper-Donets (DDB) paleorift and Peri-Caspian Basin [e.g., *Zonenshain et al.*, 1990], as schematically illustrated in Figure 13a. It has been suggested that this system represented a failed arm of a more extensive network of intracratonic rifts within a larger craton that ultimately accommodated continental breakup and development of the present southern margin of the EEC in the Devonian [e.g., *Zonenshain et al.*, 1990; cf. *Shatsky*, 1964]. Recently, various basin subsidence modeling studies of the DDB paleorift [*Kusznir et al.*, 1996a, 1996b; *Starostenko et al.*, 1999] and the implications of these studies as regards the intensity and character of Late Devonian magmatism [*Wilson and Lyashkevich*, 1996; *Wilson et al.*, 1999] suggested that mantle plume activity played a role in Late Devonian

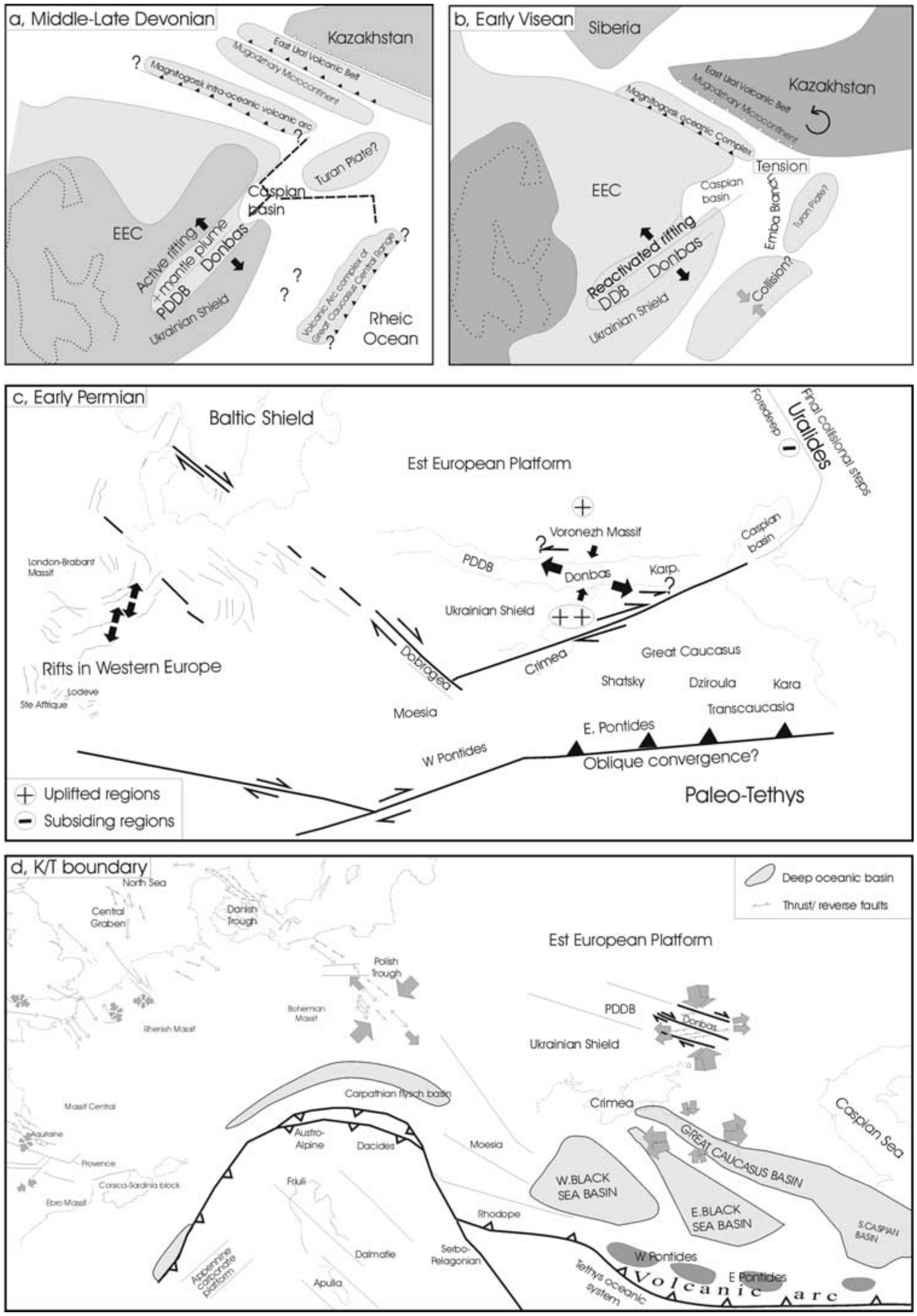

Figure 13. Schematic reconstructions with paleostress fields in the Donbas at the scale of the plate tectonics. (a) Geodynamical setting of the East European Craton in Middle Devonian times and PDDB rifting [after *Zonenshain et al.*, 1990; *Puchkov*, 1997; *Nikishin et al.*, 2001]. (b) Geodynamical setting of the East European Craton in Visean times and DDB rift reactivation [after *Zonenshain et al.*, 1990; *Puchkov*, 1997; *Brown et al.*, 1998; *Nikishin et al.*, 2001]. (c) Geodynamical setting of the East European Craton in Early Permian times and transtensional environment along the DDB [after *Ziegler*, 1990; *Puchkov*, 1997; *Nikishin et al.*, 2001]. (d) Geodynamical setting of the southern edge of the East European Platform in Late Cretaceous/Early Paleocene and tectonic inversion of the Donbas [after *Philip et al.*, 2000; *Saintot*, 2000; *Nikishin et al.*, 2001]. Couple of divergent arrows as σ_3 trend in extensional or strike-slip stress fields (from our study); couple of convergent arrows as supposed σ_1 trend in compressional or strike-slip stress fields. Abbreviations: EEC, East European Craton, PDDB, Prypriat-Dnieper-Donets Basin; Karp., Karpinsky Swell.

(“active”) rifting, supporting some earlier hypotheses [e.g., *Gavrish*, 1989; *Chekunov*, 1994].

[61] Like the Peri-Caspian basin, the DDB has often been described in the literature as a limited back arc type ocean or ocean-like basin [*Zonenshain et al.*, 1990; *Ziegler*, 1990; *Nikishin et al.*, 1996; *Sengör and Natalin*, 1996; *Golonka*, 2000] and it may be that the inferred “active” (plume-related) rifting character of the DDB may be a manifestation of “back arc” processes associated with Late Devonian subduction of oceanic lithosphere at the eastern (Uralian) and/or southern (Paleo-Tethyan/Rheic) margins of the EEC [e.g., *Fokin et al.*, 2001]. However, Urals-related subduction at this time (Late Devonian to Early Carboniferous) was eastward directed according to recent studies [*Yazeva et al.*, 1989; *Seravkin et al.*, 1992; *Puchkov*, 1997; *Chemenda et al.*, 1997; *Brown et al.*, 1998, 1999]. In this context, rifting of the DDB as a response to “back arc” processes would be related to subduction located in the present-day southern margin of the EEC and not to the Uralian geodynamics. For example, there are remnants of a Middle to Late Devonian subduction related arc complex of unknown directional affinity in the present Central Range of the Great Caucasus [*Belov*, 1981; *Milanovsky*, 1991; *Nikishin et al.*, 2001], but obviously the location of this arc complex relative to the Late Palaeozoic EEC is very speculative.

[62] These rather poorly constrained considerations of the Late Palaeozoic geodynamic setting of the DF are summarized in Figure 13a. What is important from the present paleostress study in this context is that rifting occurred (presumably in response at least in part to an “active” driving mechanism) with an extensional axis roughly perpendicular to the inferred Rheic Ocean margin of the EEC and roughly subparallel to the developing Urals orogenic belt.

[63] After a period of distinct tectonic quiescence in the latest Devonian and earliest Carboniferous, tectonic extension was clearly reactivated in the late early Visean in the DDB [*Stovba and Stephenson*, 1999] and in the DF [this study; *McCann et al.*, 2003]. The orientation of the extensional axis was similar to that of the main Late Devonian rifting stage (Figure 13b).

[64] During Early Carboniferous times, according to many authors [e.g., *Belov*, 1981; *Zonenshain et al.*, 1990; *Adamia*, 1991; *Milanovsky*, 1991; *Ustaomer and Robertson*, 1997], the “southern” margin of the EEC was part of an accretionary belt with widespread thrusting and folding (e.g., “Scythian Orogen” [*Nikishin et al.*, 2001]). However, the compressive far-field effects of this are not in evidence in the DF paleostress history (or in the preserved geological record of the DDB). Thus, for some reason the DF was isolated from the effects of Late Palaeozoic convergence processes involving the presumed orogenic consolidation to its south. One implication is that accretion of Scythian terranes to the EEC did not occur at this time; if it did, then it occurred in an extremely “soft” manner without the transmission of significant compressional stress into the EEC [*Stephenson et al.*, 2001].

[65] The “eastern” margin of the EEC in the Late Palaeozoic is much better known than the “southern” margin. In this case, compressional deformation structures began to be formed in the southern Urals at late Famennian-Early Carboniferous times with the accretion of Magnitogorsk volcanic arc [e.g., *Zonenshain et al.*, 1990; *Puchkov*, 1997; *Brown et al.*, 1998, 1999; *Brown and Spadea*, 1999] and the development of the Emba Branch of the Variscan Uralian orogenic belt [*Puchkov*, 1997]. According to *Brown et al.* [1998, 1999] and *Brown and Spadea* [1999], the arc-continent collision ended during the Tournaisian, as marked by the collapse of the accreted arc and deposition of carbonates on top of it. Thus, it appears as though the “eastern” margin of the EEC was tectonically quiescent when the Visean extensional reactivation of the DDB and Donbas rift occurred.

[66] Further to the east, however, convergence between the EEC and Kazakhstan plates continued, with the subduction of an oceanic plate (the “Paleo-Uralian Ocean” [*Puchkov*, 1991, 1997]) beneath Kazakhstan (or beneath previously accreted outboard terranes at its margin [*Puchkov*, 1997]). Figure 13b shows a schematic reconstruction of the paleotectonic setting of the time, including a speculative location of the active subduction zone, prior to Middle Carboniferous to Late Permian-Early Triassic continental collision between the EEC and Kazakhstan [*Puchkov*, 1991, 1997]. *Puchkov* [1997] mentioned that the Kazakhstan plate rotated several degrees anti-clockwise at Visean-early Bashkirian times, just preceding the “rigid” continental collision. The effect of this was to create a tensional regime in the southern part of the Urals, with “the formation of sedimentary and magmatic complexes atypical of collision or subduction” [*Puchkov*, 1997, p. 226]. Given that this tensional event in the southern Urals is contemporaneous with reactivation of extension in the interior of the EEC plate, as documented in the DDB-DF rift, it is permissible to suggest that there may be some connection. What may be important in this regard is that the residual effects of Late Devonian rifting (thermal perturbation and incompletely relaxed ambient extensional stresses) in the DDB-DF system at this time will have remained very significant. It follows that the additional imposition of even relatively small extensional stresses, such as those produced by rotation of the Kazakhstan plate relative to the EEC, could be sufficient for extensional reactivation of the DDB-DF.

[67] In Early Permian times, the Donbas was in a transtensional stress regime (Figure 13c), similar to the widespread extensional-transtensional regime that characterized most of north central Europe and the Tornquist-Tesseyre Zone at the same time [*Ziegler*, 1990]. According to *Ziegler* [1990], Late Carboniferous-Early Permian dextral translation between Africa(-Gondwana) and Laurasia was responsible for the development of regional wrench fault systems in which pull-apart basins formed, including the Permian basins of north central Europe [cf. *van Wees et al.*, 2000]. This system of regional right-lateral faults defined a diffuse plate boundary between Africa and Laurasia. The widespread tectonic instability that developed in northwestern Europe during the Late Carboniferous-Early Permian is often ascribed to the “post-orogenic extensional collapse” of the Variscan Orogeny [cf. *Ziegler*, 1990]. However, the fact that the DF (and DDB), located within the EEC and obviously not part of the Variscan belt, appear to share

this regional tectonic setting suggests otherwise. As such, the DF paleostress observations support the results of modeling studies that suggest that gravitational instability of the Variscan Orogeny would be insufficient in itself to generate the intensity and degree of post-Variscan extension observed in north central Europe [*Henk*, 2000]. Thus, the observed Early Permian state of stress of the DF developed within a widespread geodynamic setting that was related to large-scale plate boundary forces affecting much of the European lithosphere at that time.

[68] Contemporaneously, in a background of global relative sea level fall [*Harland et al.*, 1990], the Donbas, especially its southern margin and the adjacent Azov Massif and Ukrainian Shield, was affected by a very rapid, important and absolute uplift [*Stephenson et al.*, 2001]. Given the observed transtensional stress regime, this can be related to regional strike-slip movements at adjacent sub-plate boundaries. Unfortunately, there exists very little real constraint on what the paleotectonic situation in the region just to the (present-day) south of the DF was at this time. As such, it can only be speculated that such movements could have occurred between consolidated terranes to the south and the EEC itself, and/or between accreted terranes and the subducting Paleo-Tethys oceanic plate, and/or along suture zones between different terranes (cf. Figure 13c). In any case, the implication of such a model is that the southern boundary of the EEC could be considered as a broad transcurrent plate boundary at this time, similar as proposed by *Arthaud and Matte* [1977] 25 years ago from the western Variscan system (the Appalachians) to the Urals. (It is also noted that, at Wordian times, *Gaetani et al.* [2000] infer a right-lateral strike-slip boundary between western Europe (-Laurasia) and Africa (-Gondwana), as the continuation of the Paleo-Tethyan subduction zone the plate boundary.)

[69] Mesozoic tectonic stress regimes affecting the DF were related to the active southern (Tethyan) margin of the EEC [e.g., *Stampfli et al.*, 1991; *Dercourt et al.*, 1993; *Ricou*, 1996] since significant plate-scale tectonic activity in the southern Urals had ceased by the end of the Permian [*Zonenshain et al.*, 1990; *Nikishin et al.*, 1996; *Puchkov*, 1997]. The third stress regime observed in the DF (strike-slip; Figure 12c) is poorly constrained in age but could be a record of Triassic-Jurassic Eo-Cimmerian tectonics. Rift systems on the southern margins of the EEC have been inverted at the end of the Triassic, during the closure of the Paleo-Tethys ocean [*Sengör*, 1984; *Nikishin et al.*, 2001]. According to the stress orientations determined for the Donbas, the (speculative) Eo-Cimmerian event, deformation would have been (left-lateral?) transpressional indicating oblique convergence.

[70] The regional tectonic setting in which the youngest, transpressional, stress regime of the DF was formed, during Eo-Alpine deformation at end of Cretaceous-beginning of Tertiary times is shown in Figure 13d. Tectonic inversion of sedimentary basins elsewhere in Europe, such as in the Polish Trough [*Stephenson et al.*, 2003], occurred at the same time [cf. *Ziegler*, 1990]. The exact mechanism by which plate boundary stresses are transmitted into plate interiors to produce intraplate inversion structures remains unclear [e.g., *Ziegler et al.*, 1998] but, in any case, it seems highly likely that a common, plate-scale, process is responsible. Nevertheless, there is a change of trajectory of paleostress axes observed in various locations throughout Europe at this time, for example, from a slightly NW to north directed main compressional axis in the DF to a more NE directed compressional axis in the Polish Trough (Figure 13d) [*Lamarche et al.*, 1999; *Philip et al.*, 2000]. Finally, it is perhaps noteworthy that this was also the time when the extensional East Black Sea basin was developing [*Finetti et al.*, 1988; *Robinson et al.*, 1996]. Surrounding areas such as the western Caucasus are characterized by related transtensional structures of this age [*Saintot*, 2000; *Saintot and Angelier*, 2002]. Interestingly, the stress axis trends of the transpressional strike-slip stress field of the DF are identical to those of the transtensional strike-slip stress field related to East Black Sea basin opening recorded in the western Caucasus (Figure 13d) [*Saintot*, 2000; *Saintot and Angelier*, 2002].

6. Conclusion

[71] The main conclusions that can be drawn from the inferred paleostress history of the DF as reported here are: (1) The ‘‘inversion’’ of the DF, with concomitant shortening and development of compressional structures such as thrusts and folds can be reassigned to the Late Cretaceous. This is clearly not a Permian event as has been conventionally reported in the literature. (2) A strike-slip regime, probably transtensional in style, affected the DF during the Permian, contemporaneously with a regional sea level drop and uplift of the southern margin of the DF. (3) The Devonian and Early Carboniferous rifting phases characterizing the DF and Dnieper-Donets Basin occurred under an extensional stress regime without evidence of any strike-slip component along the WNW-ESE marginal faults of rift system. (4) The earliest set of WNW-ESE striking ‘‘folds’’ (the MA and open synclines and anticlines south and north) observed in the present-day structure of the DF have developed under a strike-slip regime with probable transtensional deformation, in conjunction with salt tectonics in the Permian time. (5) The second set of folds is characterized by various strikes of fold axes and is commonly associated with shallow thrusting. It corresponds to Eo-Alpine compressional and strike-slip stress fields, clearly recognized in Carboniferous and Cretaceous rocks. (6) A strike-slip regime with an E-W compressional axis can characterize a Cimmerian phase of deformation; if not, deviation of stress trends of the Eo-Alpine stress field. (7) The timing and style of tectonic events recorded by kinematic indicators in the DF permit important new constraints to be placed on the otherwise poorly known geodynamic history of the southeastern margin of Europe.

[72] **Acknowledgments.** The study was carried on in the framework of EUROPROBE’s Georift/INTAS 97-0743 project. We warmly thank field trip participants and especially Alexander Kitchka for their logistical support and fruitful geological discussions on the outcrops. We also wish to thank A. M. Nikishin and an anonymous reviewer for their comments on the manuscript. The present manuscript is Netherlands Research School of Sedimentary Geology contribution number 20030411. The first author is supported by a grant from the Netherlands Research Foundation (NWO).

References

Adamia, S. A., The Caucasus Oil and gas province, *Occasional Publications, ESRI, New Ser. 7*, part I, pp. 53–74, Earth Sci. and Resour. Inst., Univ. of S. Carolina, Columbia, 1991.

Alexandre, P., A. Saintot, J. Wijbrans, R. Stephenson, M. Wilson, A. Kitchka, and F. Chalot-Prat, $^{40}Ar/^{39}Ar$ dating of magmatic activities in the Donbas Foldbelt and the Scythian Platform (Eastern Europe) indicating a possible mantle plume source, *Geophys. Res, Abstr.*, *5*, 01506, 2003.

Angelier, J., Inversion of field data in fault tectonics to obtain the regional stress: A new rapid direct inversion method by analytical means, *Geophys. J. Int.*, *103*, 363–376, 1990.

Angelier, J., Palaeostress analysis of small-scale brittle structures, in *Continental Deformation*, edited by P. Hancock, pp. 53–100, Pergamon, New York, 1994.

Angelier, J., B. Colletta, and R. E. Anderson, Neogene paleostress changes in the Basin and Range: A case study at Hoover Dam, Nevada-Arizona, *Geol. Soc. Am. Bull.*, *96*, 347–361, 1985.

Arthaud, F., and P. Matte, Late Paleozoic strike-slip faulting in southern Europe and northern Africa: Result of a right-lateral shear zone between the Appalachians and the Ural, *Geol. Soc. Am. Bull.*, *88*, 1305–1320, 1977.

Balukhovsky, N. F., Geological structure and prospects of oil/gas content in western and northern margins of the Donbas (in Russian), *Iz. Acad. Sci. Ukraine*, 156 pp., 1959a.

Balukhovsky, N. F., New data about geological structure and development of the Donets Basin margins (in Russian), *Izv. Akad. Nauk USSR*, *2*, 34–41, 1959b.

Belichenko, P. V., O. B. Gintov, V. V. Gordienko, V. A. Korchemagin, B. S. Panov, I. A. Pavlov, and O. V. Usenko, Main stages of Olkhovatsko-Volyntsevskaya Anticline evolution in Donbas in connection with its ore potential according to tectonophysical, geothermal and gravimetric data (in Russian), *Geophys. J.*, *21*, 69–84, 1999.

Belokon, V. G., Deep structure of the Donbas (in Russian), *Geol. J.*, *5*, 10–25, 1975.

Belov, F. A., Geological description of the Rostov, Volgograd, Astrakhan' regions and Kalmyk ASSR (in Russian), in *Geology of the USSR*, vol. 46, *Rostov, Volgograd, Astrakhan and Kalmyk Regions*, edited by F. A. Belov, 667 pp., Minist. of Geol. of the USSR, Volgo, 1970.

Belov, A. A., Tectonic development of the Alpine fold area in the Paleozoic (in Russian), 212 pp., Nauka, Moscow, 1981.

Bergerat, F., Stress fields in the European platform at the time of Africa-Eurasia collision, *Tectonics*, *6*, 99–132, 1987.

Borodulin, M. I., New approach of regional seismic investigations tecnigues and geological referencing of interfaces in the Dniepr basin (in Rusian), *Geophys. Collect.*, *60*, 9–17, 1974.

Brem, A., Using deviations in local stress patterns to deduce the geometry of the eastern part of the Styla Horst, Donbas Foldbelt, Ukraine, internal report, 42 pp., Vrije Univ., Amsterdam, 2000.

Brown, D., and P. Spadea, Processes of forearc and accretionary complex formation during arc-continent collision in the Southern Ural Mountains, *Geology*, *27*(7), 649–652, 1999.

Brown, D. L., C. Juhlin, J. Alvarez-Marron, A. Perez-Estaun, and A. Oslianski, Crustal-scale structure and evolution of an arc-continent collision zone in the Southern Urals, Russia, *Tectonics*, *17*, 158–171, 1998.

Brown, D., J. Alvarez-Marron, A. Perez-Estaun, V. Puchkov, and C. Ayala, Basement influence on foreland thrust and fold belt development: An example from the southern Urals, *Tectonophysics*, *308*, 459–472, 1999.

Chekunov, A. V., The geodynamics of the Dniepr-Donets rift syneclise (in Russian), *Geophys. J.*, *16*, 3–13, 1994.

Chekunov, A. V., and V. V. Naumenko, The relationship between the deep crustal rearrangement, tectonic movements, magmatism, metamorphism and metal content in the Dnieper-Donets Paleorift (in Russian), *Geophys. J.*, *4*, 25–34, 1982.

Chekunov, A. V., L. T. Kaluzhnaya, and L. I. Ryabchun, The Dniepr-Donets paleorift, Ukraine: Deep structures and hydrocarbon accumulations, *J. Pet. Geol.*, *16*, 183–196, 1993.

Chemenda, A., P. Matte, and V. Sokolov, A model of Paleozoic obduction and exhumation of high pressure/low temperature rocks in the southern Urals, *Tectonophysics*, *276*, 217–227, 1997.

Chirvinskaya, M. V., and V. B. Sollogub, Deep structure of the Dniepr-Donets Aulacogen from geophysical data (in Russian), 178 pp., Naukova Dumka, Kiev, Russia, 1980.

Dercourt, J., L.-E. Ricou, and B. Vrielynck (Eds.), Atlas Tethys, Palaeoenvironmental maps, 307 pp., 14 maps, 1 plate, Gauthier-Villars, Paris, 1993.

Donetsk State Regional Geological Survey, Geological map of the Ukrainian Donbas Foldbelt, scale 1:200000, Ukraine, 1995.

Dvorjanin, E. S., A. P. Samoyluk, M. G. Egurnova, N. Y. Zaykovsky, Y. Y. Podladchikov, F. J. G. van den Belt, and P. L. de Boer, Sedimentary cycles and paleogeography of the Dnieper Donets Basin during the late Visean-Serpukhovian based on multiscale analysis of well logs, *Tectonophysics*, *268*, 169–187, 1996.

Eisenverg, D. E., (Ed.), *Geology and Oil and Gas Occurrences of the DnieperDonets Depression*: *Stratigraphy*, 148 pp., Naukova Dumka, Kiev, Russia, 1988.

Finetti, I. R., G. Bricchi, A. Del Ben, M. Pipan, and Z. Xuan, Geophysical study of the Black Sea, in *Monograph of the Black Sea*, edited by I. R. Finetti, *Boll. Geofis. Teor. Appl.*, *30*, ((117–118)), 197–324, 1988.

Fokin, P. A., A. M. Nikishin, and P. A. Ziegler, Peri-Uralian and Peri-Palaeo-Tethyan rift systems of the East European Craton, in *Peri-Tethys Memoir 6: Peri-Tethyan Rift/Wrench Basins and Passive Margins*, edited by P. A. Ziegler et al., *Mém. Mus. Natl. Hist. Nat. Ser. C Paris*, *186*, 347–368, 2001.

Gaetani, M., et al., Wordian, in *Atlas Peri-Tethys, Palaeogeographic Maps*, edited by J. Dercourt et al., map 3, Comm. de la Carte Géol. du Monde/Comm. for the Geol. Map of the World (CCGM/CGMW), Paris, 2000.

Garetsky, R. G., *Tectonics of Young Platforms of Eurasia* (in Russian), 210 pp., Nauka, Moscow, 1972.

Garkalenko, I. A., M. I. Borodulin, and A. K. Mikhalev, About the transition zone between the Dniepr-Donets Basin and Donets folded structure (in Russian), *Geol. J.*, *31*, 92–98, 1971.

Gavrish, V. K., Depth structure and evolution of the Pripyat-Dniepr-Donets and Kenyan rifts (in Russian), *Geol. J.*, *45*, 10–18, 1985.

Gavrish, V. K., (Ed.), *Geology and Oil and Gas Potential of the Dniepr-Donets Depression, Depth Structure and Geotectonic Evolution* (in Russian), 208 pp., Naukova Dumka, Kiev, Russia, 1989.

Golonka, J., Cambrian-Neogene plate tectonic maps, 125 pp., Jagiellonian Univ., Krakow, 2000.

Harland, W. B., R. L. Armstrong, A. V. Cox, L. E. Craig, A. G. Smith, and D. G. Smith, *A Geologic Time Scale 1989*, 263 pp., Cambridge Univ. Press, New York, 1990.

Henk, A., Foreland-directed lower-crustal flow and its implications for the exhumation of high-pressure-high-temperature rocks, in *Orogenic Processes: Quantification and Modelling in the Variscan Belt*, edited by F. Wolfgang et al., *Geol. Soc. Spec. Publ.*, *179*, 355–368, 2000.

Hippolyte, J.-C., and M. Sandulescu, Paleostress characterization of the "Wallachian Phase" in its type area (southeastern Carpathians, Romania), *Tectonophysics*, *263*, 235–248, 1996.

Izart, A., C. Briand, D. Vaslet, D. Vachard, R. Coquel, and A. Maslo, Stratigraphy and sequence stratigraphy of the Moscovian in the Donets basin, *Tectonophysics*, *268*, 189–209, 1996.

Konashov, V. C., Expression of an Early Cimmerian folding phase in the Donets Basin (in Russian), *Geotectonics*, *4*, 29–36, 1980.

Korchemagin, V. A., and V. S. Yemets, Distinctive features of development of the tectonic structure and stress fields of the Donets basin and the Eastern Azov region, *Geotectonics*, *21*, 231–237, 1987.

Kusznir, N. I., A. Kovkhuto, and R. A. Stephenson, Syn-rift evolution of the Pripyat Trough, constraints from structural and stratigraphic modelling, *Tectonophysics*, *268*, 221–236, 1996a.

Kusznir, N. I., S. Stovba, R. A. Stephenson, and K. N. Poplavsky, The formation of the N. W. Dnieper-Donets Basin, 2D forward and reverse syn-rift and post-rift modelling, *Tectonophysics*, *268*, 237–255, 1996b.

Lamarche, J., J.-L. Mansy, F. Bergerat, O. Averbuch, M. Hakenberg, M. Lewandowski, E. Stupicka, J. Swidrowska, B. Wajsprych, and J. Wieczorek, Variscan tectonics in the Holy Cross Mountains (Poland) and the role of structural inheritance during Alpine tectonics, *Tectonophysics*, *313*, 171–186, 1999.

Levenshtein, M. L., Analysis of thickness variations of Carboniferous sediments in the Donets Basin (in Russian), in *Geology of Coal and Oil Shale Deposits of the USSR 1*, pp. 213–233, Nedra, Moscow, 1963.

Lutuguin, L. I., Selected works on the geology of the Donets basin (in Russian), edited by I. T. Shvets and Ye. O. Novik, 218 pp., UkrSSR Acad. Sci., Kiev, Russia, 1956.

McCann, T., A. Saintot, F. Chalot-Prat, A. Kitchka, P. Fokin, A. Alekseev, and EUROPROBE-INTAS Research Team, Evolution of the southern margin of the Donbas (Ukraine) from Devonian to Early Carboniferous times, in *Tracing Tectonic Deformation Using the Sedimentary Record*, edited by T. McCann and A. Saintot, *Geol. Soc. Spec. Publ.*, *208*, 1–28, 2003.

Maidanovich, I. A., and A. Y. Radzivill, Tectonic peculiarities of Ukraine's coal basins (in Russian), 120 pp., Naukova Dumka., Kiev, Russia, 1984.

Maystrenko, Y., et al., Crustal-scale pop-up structure in cratonic lithosphere: DOBRE deep seismic reflection study of the Donbas fold belt, Ukraine, *Geology*, *31*(8), 733–736, 2003.

Mercier, J. L., D. Sorel, and K. Simeakis, Changes in the state of stress in the overriding plate of a subduction zone: The Aegean Arc from the Pliocene to the Present, *Ann. Tectonicae*, *1*(1), 20–39, 1987.

Mikhalev, A. K., and M. I. Borodulin, On the deep structure of the Donets Basin in the light of recent geophysical data (in Russian), *Geotectonics*, *5*, 49–57, 1976.

Milanovsky, E. E., *Geology of the USSR*, part 3 (in Russian), 272 pp., Moscow Univ. Press, Moscow, 1991.

Milanovsky, E. E., Aulacogens and aulacogeosynclines, regularities in setting and evolution, *Tectonophysics*, *215*, 55–68, 1992.

Muratov, M. V., Main types of depressions of ancient platforms and the problem of their origins (in Russian), *Bull. Moscow Soc. Nat. Geol. Sect.*, *5*, 61–71, 1972.

Nalivkin, D. V., (Ed.), Geological map of the U.S.S.R. and adjoining water-covered areas, scale 1:2,500,000, compiled by A. P. Karpinsky All-Union Geol. Res. Inst. (VSEGEI), Editor-in-Chief R. I. Sokolov, Minist. of Geol. of the USSR, 1983.

Nikishin, A. M., et al., Late Precambrian to Triassic history of the East European Craton: Dynamics of sedimentary basin evolution, *Tectonophysics*, *268*, 23–63, 1996.

Nikishin, A. M., P. A. Ziegler, D. I. Panov, B. P. Nazarevich, M.-F. Brunet, R. A. Stephenson, S. N. Bolotov, M. V. Korotaev and P. L. Tikhomirov, Mesozoic and Cenozoic evolution of the Scythian Platform-Black Sea-Caucasus domain, in *Peri-Tethys Memoir 6: Peri-Tethyan Rift/Wrench Basins and Passive Margins* edited by P. A. Ziegler, W. Cavazza, A. H. F. Robertson and S. Crasquin-Soleau, *Mém. Mus. Natl. Hist. Nat. Ser. C Paris*, *186*, 295 – 346, 2001.

Philip, J., et al., Late Maastrichtian, in *Atlas Peri-Tethys, Palaeogeographic Maps*, edited by J. Dercourt et al., map 16, Comm. de la Carte Géol. du Monde/ Comm. for the Geol. Map of the World (CCGM/ CGMW), Paris, 2000.

Pogrebitsky, Y. O., Donets coal basin (in Russian), *Chem. Solid Fuels*, *8*(5), 439 – 447, 1937.

Pogrebnov, N. I., I. A. Ocheretenko, and V. V. Trostchenko, Geological and structural map of the Donbas, scale 1:500000, in *Structural Geology of the Donets Coal Basin: Proceedings of All-Union Research Institute on Exploration of Coal Fields*, 149 pp., Minist. of Geol. of the U.S.S.R., of the Russian Socialist Fed. Sovietic Repub.), of the Socialist Sov. Repub. of Ukraine, Nedra Press, Moscow, 1985.

Popov, V. S., New data on the tectonics of the northern marginal part of the Donets Basin (in Russian), *Problems Soviet Geol.*, *12*, 1025 – 1043, 1936.

Popov, V. S., The tectonics of the Donets Basin (in Russian), report of the 17th International Geological Congress, USSR, 628 pp., Int. Geol. Congress, Moscow, 1939.

Popov, V. S., Tectonics of the Donets basin (in Russian), in *Geology of Coal and Oil Shale Deposits of the USSR 1*, pp. 103 – 151, Nedra, Moscow, 1963.

Privalov, V. A., M. V. Zhykalyak, M. A. Piskovoy, and E. A. Panova, Structural setting and principal displacement zone of the Donets Basin, Abs. EUROPROBE Workshop, Gurzuf, 12 – 16 Oct. 2000, *Geophys. J.*, *4*, 119 – 120, 2000.

Puchkov, N., The Paleozoic of the Uralo-Mongolian Fold system, *Occasional Publications: ESRI, New Ser. 7* [I-II], part I, pp. 1 – 69, Earth Sci. and Resour. Inst., Univ. of S. Carolina, Columbia, 1991.

Puchkov, V. N., Structure and geodynamics of the Uralian orogen, in *Orogeny Trough Times*, edited by J.-P. Burg and M. Ford, *Geol. Soc. Spec. Publ.*, *121*, 201 – 236, 1997.

Ricou, L.-E., The Plate Tectonic History of the Past Tethys Ocean, in *The Oceans Basins and Margins*, vol. 8, *The Tethys Ocean*, edited by A. E. M. Nairn et al., pp. 3 – 70, Plenum, New York, 1996.

Robinson, A. G., J. H. Rudat, C. J. Banks, and R. L. F. Wiles, Petroleum geology of the Black Sea, *Mar. Pet. Geol.*, *13*(2), 195 – 223, 1996.

Roy-Chowdhury, K., et al., DOBRE-2000: Deep Reflection Seismic, Gravimetric and Surface Structural Controls Across a Devonian Failed Rift in the South-eastern Europe, *Eos Trans. AGU*, *82*(47), Fall Meet. Suppl., Abstract T51B-0866, 2001.

Saintot, A., Vol 1: Reconstruction des champs de paléocontraintes de la Crimée au Caucase nord-occidental, relations avec le développement des structures majeures. Apport de la télédétection à l'analyse structurale; Vol 2: Annexes, Thèse de Doctorat, Mém. Sc. Terre No. 2010, Univ. Pierre et Marie Curie, Paris, 2000.

Saintot, A., and J. Angelier, Tectonic paleostress fields and structural evolution of the NW-Caucasus fold and thrust belt from Late Cretaceous to Quaternary, in *Paleostresses and Tectonics in the Peri-Tethyan Margins*, edited by F. Bergerat, E. Barrier, J. Angelier and J. W. Granath, Peri-Tethys Special Issue, *Tectonophysics*, *357*, 1 – 31, 2002.

Saintot, A., R. Stephenson, S. Stovba, and Y. Maystrenko, Structures associated with the inversion of the Donbas, *Tectonophysics*, *373*, 181 – 207, 2003.

Sébrier, M., J.-L. Mercier, F. Megard, G. Laubacher, and E. Carey-Gailhardis, Quaternary normal and reverse faulting and the state of stress in the central Andes of south Peru, *Tectonics*, *4*, 739 – 780, 1985.

Sengör, A. M. C., The Cimmeride orogenic system and the tectonics of Eurasia, *Spec. Pap. Geol. Soc. Am.*, *195*, 1 – 82, 1984.

Sengör, A. M. C., and B. A. Natalin, Paleotectonics of Asia: Fragment of a synthesis, in *The Tectonic Evolution of Asia*, edited by A. Yin and T. M. Harrison, pp. 486 – 640, Cambridge Univ. Press, New York, 1996.

Seravkin, I. B., A. M. Kosarev, D. N. Salikhov, S. Y. Znamensky, A. M. Rykus, Z. I. Rodicheva, *Volcanism of the Southern Urals* (in Russian), Nauka, Moscow, 1992.

Shatsky, N. S., About types of troughs like the Donetsk (in Russian), *Nauka II*, 544 – 553, 1964.

Sobornov, K., Structural evolution of the Karpinsky Swell, Russia, *C. R. Acad. Sci. Paris, Ser. II*, *321*, 161 – 169, 1995.

Sollogub, V. B., M. I. Borodulin, and A. V. Chekunov, Deep-lying structure of the Donbas and adjacent regions, *Geol. Zhur. AN UkrSSR*, *37*(2), 23 – 31, 1977.

Stampfli, G., J. Marcoux, and A. Baud, Tethyan margins in space and times, *Palaeogeogr. Palaeoclimatol. Palaeoecol.*, *87*, 373 – 409, 1991.

Starostenko, V. I., V. A. Danilenko, D. B. Vengrovitch, R. I. Kutas, S. M. Stovba, R. A. Stephenson, and O. M. Kharitonov, A new geodynamical-thermal model of rift evolution, with application to the Dnieper-Donets Basin, Ukraine, *Tectonophysics*, *313*, 29 – 40, 1999.

Stepanov, P. I., Southern Excursion, Donets Carboniferous Basin (in Russian), in *Proc. Int. Geol. Congr. 17th*, 114 pp., 1937.

Stephenson, R. A., S. M. Stovba, and V. I. Starostenko, Pripyat-Dniepr-Donets Basin: Implications for dynamic of rifting and the tectonic history of the northern Pery-tethyan Platform, in *Peri-Tethys Memoir 6: Peri-Tethyan Rift/Wrench Basins and Passive Margins*, edited by P. A. Ziegler et al., *Mém. Mus. Natl. Hist. Nat. Ser. C Paris*, *186*, 369 – 406, 2001.

Stephenson, R. A., M. Narkiewicz, R. Dadlez, J.-D. van Wees, and P. Andriessen, Tectonic subsidence modelling of the Polish Basin in the light of new data on crustal structure and magnitude of inversion, *Sediment. Geol.*, *156*, 59 – 70, 2003.

Stovba, S. M., and R. A. Stephenson, The Donbas Foldbelt: Its relationships with the uninverted Donets segment of the Dniepr-Donets Basin, Ukraine, *Tectonophysics*, *313*, 59 – 83, 1999.

Stovba, S. M., and R. A. Stephenson, Style and timing of salt tectonics in the Dniepr-Donets Basin (Ukraine): Implications for triggering and driving mechanisms of salt movement in sedimentary basins, *Mar. Pet. Geol.*, *19*, 1169 – 1189, 2002.

Stovba, S. M., R. A. Stephenson, and M. Kivshik, Structural features and evolution of the Dnieper-Donets Basin, Ukraine, from regional seismic reflection profiles, *Tectonophysics*, *268*, 127 – 147, 1996.

Stovba, S. M., Y. P. Maystrenko, R. A. Stephenson, and N. J. Kusznir, The formation of the southeastern part of the Dniepr-Donets Basin: 2-D forward and reverse modelling taking into account post-rift redeposition of syn-rift salt, *Sediment. Geol.*, *156*, 11 – 33, 2003.

Ustaömer, T., and A. H. F. Robertson, Tectonic-sedimentary evolution of the North Tethyan margin in the Central Pontides of Northern Turkey, in *Regional and Petroleum Geology of the Black Sea and Surrounding Regions*, edited by A. G. Robinson, *AAPG Mem.*, *68*, 255 – 290, 1997.

van Wees, J.-D., R. A. Stephenson, S. M. Stovba, and V. A. Shymanovskyi, Tectonic variation in the Dnieper-Donets Basin from automated modelling of backstripped subsidence curves, *Tectonophysics*, *268*, 257 – 280, 1996.

Van Wees, J.-D., R. A. Stephenson, P. A. Ziegler, U. Bayer, T. McCann, R. Dadlez, R. Gaupp, M. Narkiewicz, F. Bitzer, and M. Scheck, On the origin of the Southern Permian Basin, Central Europe, *Mar. Pet. Geol.*, *17*, 43 – 59, 2000.

Wilson, M., and Z. M. Lyashkevich, Magmatism and the Geodynamics of rifting of the Pripyat-Dnieper-Donets rift, East European Platform, *Tectonophysics*, *268*, 65 – 81, 1996.

Wilson, M., J. Wijbrans, P. A. Fokin, A. M. Nikishin, V. I. Gorbachev, and B. P. Nazarevich, $^{40}Ar/^{39}Ar$ dating, geochemistry and tectonic setting of the Early Carboniferous dolerite sills in the Pechora basin, foreland of the Polar Urals, *Tectonophysics*, *313*, 107 – 118, 1999.

Yazeva, R. G., V. N. Puchkov, and V. V. Bochkarev, Relics of the active continental margin in the Urals (in Russian), *Geotektonika*, *3*, 76 – 85, 1989.

Zhykalyak, M. V., V. A. Privalov, L. I. Ilnitsky, and E. A. Panova, Relationships between Hercynian, Cimmerian and Alpine deformation patterns in the Donets Foldbelt, Abs. EUROPROBE Workshop, Gurzuf, 12 – 16 Oct. 2000, *Geophys. J.*, *4*, 143 – 144, 2000.

Ziegler, P. A., *Geological Atlas of Western and Central Europe*, 2nd ed., 239 pp., Shell Int. Pet. Maatschappij. B. V., New York, 1990.

Ziegler, P. A., J.-D. Van Wees, and S. A. P. L. Cloetingh, Mechanical controls on collision-related compressional intraplate deformation, *Tectonophysics*, *300*, 103 – 129, 1998.

Zonenshain, L. P., M. I. Kuzmin, and L. M. Natapov, *Geology of the USSR: A Plate- Tectonic Synthesis*, *Geodyn. Ser.*, vol. 21, edited by B. M. Page, 242 pp., AGU, Washington, D. C., 1990.

A. Brem, A. Saintot, and R. Stephenson, Faculty of Earth and Life Sciences, De Boelelaan 1085, NL-1081 HV Amsterdam, Netherlands. (saia@geo.vu.nl)

V. Privalov, Faculty of Mining and Geology, Donetsk State Technical University, 58 Artyom Street, 83000 Donetsk, Ukraine.

S. Stovba, Technology Centre, Ukrgeofisika, 10, S. Perovska, Kyiv 03057 Ukraine.